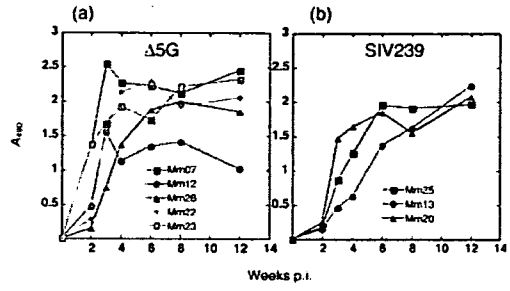


**Fig. 3.** Anti-gp120 Ab responses. Anti-gp120 Ab responses in Δ5G-infected (a) and SIV239-infected (b) animals were indicated as $A_{490}$ using plasma diluted 1 : 100 in an ELISA.

peaked at 3–4 weeks p.i. in Δ5G-infected animals (Fig. 3a), those in SIV239-infected animals remained generally lower and required longer periods of time to reach their peak (Fig. 3b). Of note, whilst anti-gp120 Ab responses did not correlate well with nAb titres in the chronic phase in Δ5G-infected animals, the hierarchy detected in nAb titres (Mm07, Mm22, Mm23, Mm12 and Mm26, in descending order) was similar to that observed for gp120-binding antibodies at 2 weeks p.i. (Fig. 3a).

## Ab responses to linear epitopes in gp120 and gp41 in Δ5G-infected animals differ from those detected in SIV239-infected animals

Next, we examined Ab-binding responses to linear epitopes in plasma samples from infected animals at 8 weeks p.i., as both nAb and anti-gp120-binding Ab were detected at this time point (Figs 2 and 3). We used 72 overlapping peptides encompassing the entire Env sequence of SIV239 for the detection of epitope-specific Ab in plasma samples from Δ5G-infected or SIV239-infected animals. As shown in Fig. 4 and Table 1, the plasma samples reacted with the peptides in six regions: two in gp120 and four in gp41. The regions in gp120 resided in the vicinity of V1/V2, designated region 1 (aa 109–193), and at the C terminus, designated region 2 (aa 493–529). Of note, only linear region 1 was directly affected by selected deglycosylation (aa 146 and 171). The regions in gp41 were located in the ectodomain for region 3 (aa 589–625) and region 4 (aa 660–685), and in the cytoplasmic domain for region 5 (aa 721–757) and region 6 (aa 841–879).

Although Ab responses to most of the peptides recognized in the plasma samples from Δ5G-infected animals were similar to those in SIV239-infected animals, a few peptides were recognized by Abs only in samples from Δ5G-infected animals, and Ab reactivity to some peptides was significantly different between the two groups (Fig. 4b, c and Table 1). Firstly, in region 1, whereas five peptides (Env-10, -12, -13, -14 and -15) were recognized by Abs from Δ5G-infected animals, only three peptides (Env-10, -12 and -13) reacted with Abs from SIV239-infected animals (Fig. 4b and c). Peptide Env-10 was detected by Abs from four Δ5G-infected animals, but from only one of the SIV239-infected animals. Similarly, peptides Env-12 and -13 were detected by Abs from five Δ5G-infected animals and two SIV239-infected animals. In contrast, peptides Env-14 and -15 were detected by Abs from Δ5G-infected animals but not SIV239-infected animals. The specificity of Δ5G infection in the reactivity of peptide Env-14 was statistically significant ($P$=0.0149) (Table 1). Secondly, the reactivity of Ab from Δ5G-infected animals with the peptides in regions 2, 3 and 4 was lower than that recorded with Ab from SIV239-infected animals (Fig. 4b and c). As shown in Table 1, the reduction in Ab reactivity from Δ5G-infected animals to peptide Env-51 (region 3) and peptide Env-56 (region 4) was significant ($P$=0.014 and 0.0053, respectively); however, the reduction in Ab response in region 2 was not significant. In addition, there were no significant differences in the Ab responses to the peptides in regions 5 and 6 between Δ5G-infected and SIV239-infected monkeys (Fig. 4b, c and Table 1).

## A Δ5G-specific linear epitope resides in the region containing the third deglycosylation site (aa 171) between V1 and V2

As region 1 also contained the site of two mutations introduced to limit glycosylation in the Δ5G mutant, we focused additional studies on this region. To identify the Δ5G-specific epitope(s) in region 1, peptide ELISA was performed with 12 newly synthesized shorter peptides based on the Δ5G sequence spanning the V1/V2 region (Fig. 5). Ab reactivity to peptide Env-14 was mapped to peptides V1V2-9–11 (Fig. 5a). Thus, three linear epitopes (encompassed in peptides Env-10, V1V2-3 and V1V2-9–11) were identified within the V1/V2 region (Figs 4 and 5). Whilst two epitopes contained in peptides Env-10 and V1V2-3 were recognized by Ab from both SIV239- and Δ5G-infected animals, the epitope(s) corresponding to peptides V1V2-9–11 was specific to Δ5G infection (Fig. 5a). As the latter contained the third deglycosylation mutation (Figs 1 and 5b, aa 171), Δ5G specificity was probably secondary to the removal of *N*-glycan at this site in SIV239 gp120 (Fig. 5).

## Δ5G-specific Ab responses to linear epitopes in Env elicited immediately following primary infection

In an effort to define the potential relevance of the linear epitope-specific Ab responses in the reduction of acute virus replication in Δ5G-infected animals, we examined the kinetics of Ab reactivity to 12 peptides: Env-10, V1V2-3 and V1V2-9, -10 and -11 for epitopes in region 1; Env-42 and -43 for epitopes in region 2; Env-50 and -51 for epitopes in region 3; Env-56 for epitopes in region 4; and Env-61 and -62 for epitopes in region 5 (Fig. 6). Whilst the induction kinetics of Ab to most peptides were variable in

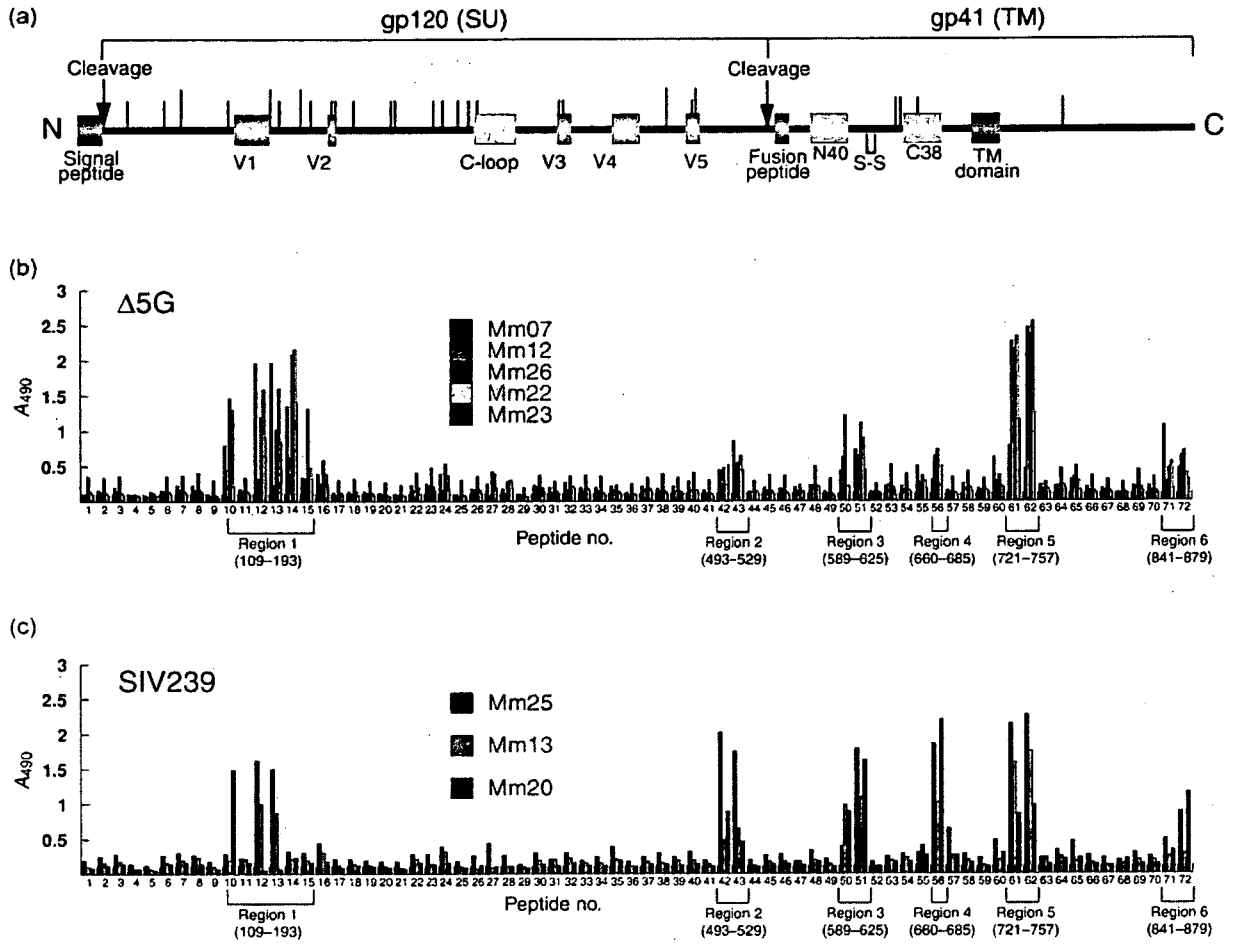


**Fig. 4.** Ab reactivity to synthetic overlapping peptides spanning the entire Env protein. (a) Diagram of SIV239 Env with the locations of the signal peptide (violet box), variable regions (pink boxes), cysteine loop (yellow box), fusion peptide (green box), N-terminal (N40) and C-terminal (C38) heptad repeats (light-blue boxes), membrane-spanning domain (blue box) and *N*-glycosylation sites (vertical bars) (Burns & Desrosiers, 1991; Choi *et al.*, 1994; Liu *et al.*, 2002). Red vertical bars indicate deglycosylation sites (aa 79, 146, 171, 460 and 479) in Δ5G. S-S indicates the indispensable disulfide bond for hairpin loop formation of the TM protein. (b, c) Plasma samples collected from animals infected with Δ5G (b) and SIV239 (c) at 8 weeks p.i. were used to examine Ab reactivity to 72 peptides (25 mers) overlapping by 13 residues each and spanning the entire Env protein. Reactivity was shown by $A_{490}$.

plasma from both groups of animals, Ab to V1V2-9, -10 and -11 was specific for Δ5G-infected animals, with rapid induction following primary infection. Ab responses to Env-61 and -62 were also induced rapidly in animals from the two groups; however, it has already been confirmed by SIV and HIV studies that a linear epitope covered by these peptides is the immunodominant epitope with no association with virus control (Eberle *et al.*, 1997; Kent *et al.*, 1992). In contrast to Ab responses to V1/V2 peptides, whilst Ab to peptides Env-51 and -56 in the gp41 ectodomain were detected in SIV239-infected animals, these reactions were low until at least 12 weeks p.i. in Δ5G-infected animals.

## Properties of Ab against Δ5G-specific linear epitope

Although Ab reactivity to peptide V1V2-9, -10 and -11 was elicited specifically in Δ5G-infected animals, these Abs were non-nAbs, as these binding Abs were detected in all Δ5G-infected animals, including a nAb-undetectable monkey (Mm26), and before nAb was detected. In addition, we attempted to inhibit neutralization by the addition of excess concentrations of V1V2-9, -10 and -11 to the neutralization assay performed with plasma from Δ5G-infected animals collected at 8 and 12 weeks p.i. The reduction of nAb by the addition of an excess amount of

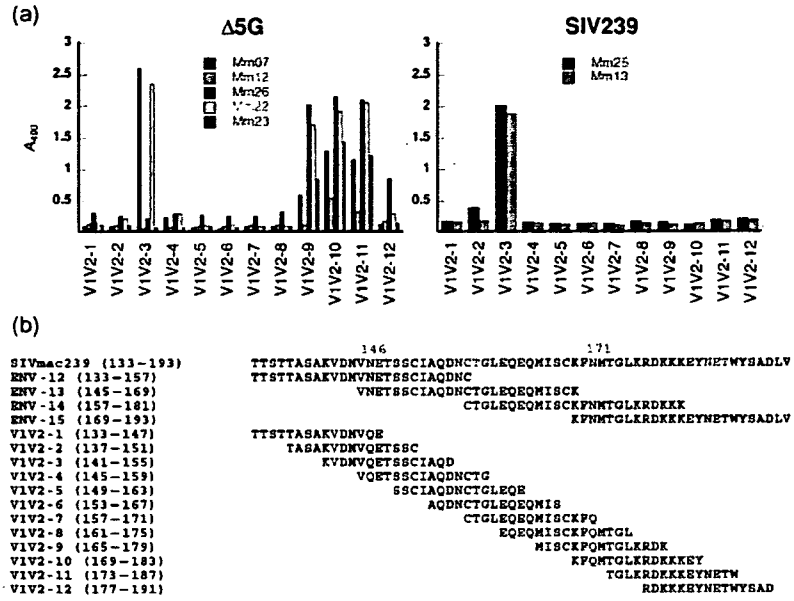


**Fig. 5.** Ab reactivity to linear epitopes in the V1/V2 region of gp120. (a) To define linear epitopes in the V1/V2 region, peptide ELISA was performed using 12 peptides (15 mers) overlapping by 11 residues each. (b) Sequences and positions of the 12 V1/V2 peptides used in (a) and the peptides Env-12 to -15.

peptide was not detected in any samples, confirming that the epitopes targeted by nAb and V1V2-specific Ab were distinct (data not shown).

Next, we tested plasma IgG samples from SIV-infected animals for the quantitative capture of whole virions. IgG fractions of plasma samples from SIV-infected animals collected at 3–4 weeks p.i. were compared for their capacity to capture Δ5G or SIV239 virions. IgG fractions from two Δ5G-infected animals (Mm07 and Mm22) exhibited remarkably higher virion capture activity than those from other animals (Fig. 7a); however, this capture activity was

**Table 1.** Epitope-specific Ab-binding regions in Env and influence of deglycosylation on Ab binding

| Env subunit | Ab-binding region | Peptide no. | Amino acid range | Region | *P* value* |
|---|---|---|---|---|---|
| SU | Region 1 | 10 | 109–133 | V1 | 0.6733 |
| | | 12 | 133–157 | V1 | 0.5678 |
| | | 13 | 145–169 | V1/V2 | 0.5563 |
| | | 14 | 157–181 | V1/V2 | 0.0149† |
| | | 15 | 169–193 | V1/V2 | 0.2385 |
| | Region 2 | 42 | 493–517 | SU C terminus | 0.0822 |
| | | 43 | 505–529 | | 0.3039 |
| TM | Region 3 | 50 | 589–613 | Ectodomain | 0.4791 |
| | | 51 | 601–625 | | 0.0140† |
| | Region 4 | 56 | 660–685 | Ectodomain | 0.0053‡ |
| | Region 5 | 61 | 721–746 | Cytoplasmic domain | 0.6818 |
| | | 62 | 732–757 | | 0.8188 |
| | Region 6 | 71 | 841–865 | Cytoplasmic domain | 0.5237 |
| | | 72 | 853–879 | | 0.2451 |

*A *t*-test was performed by using data in Fig. 4 to determine differences in Ab reactivity between SIV239 infection and Δ5G infection.
†$P<0.05$; ‡$P<0.01$.

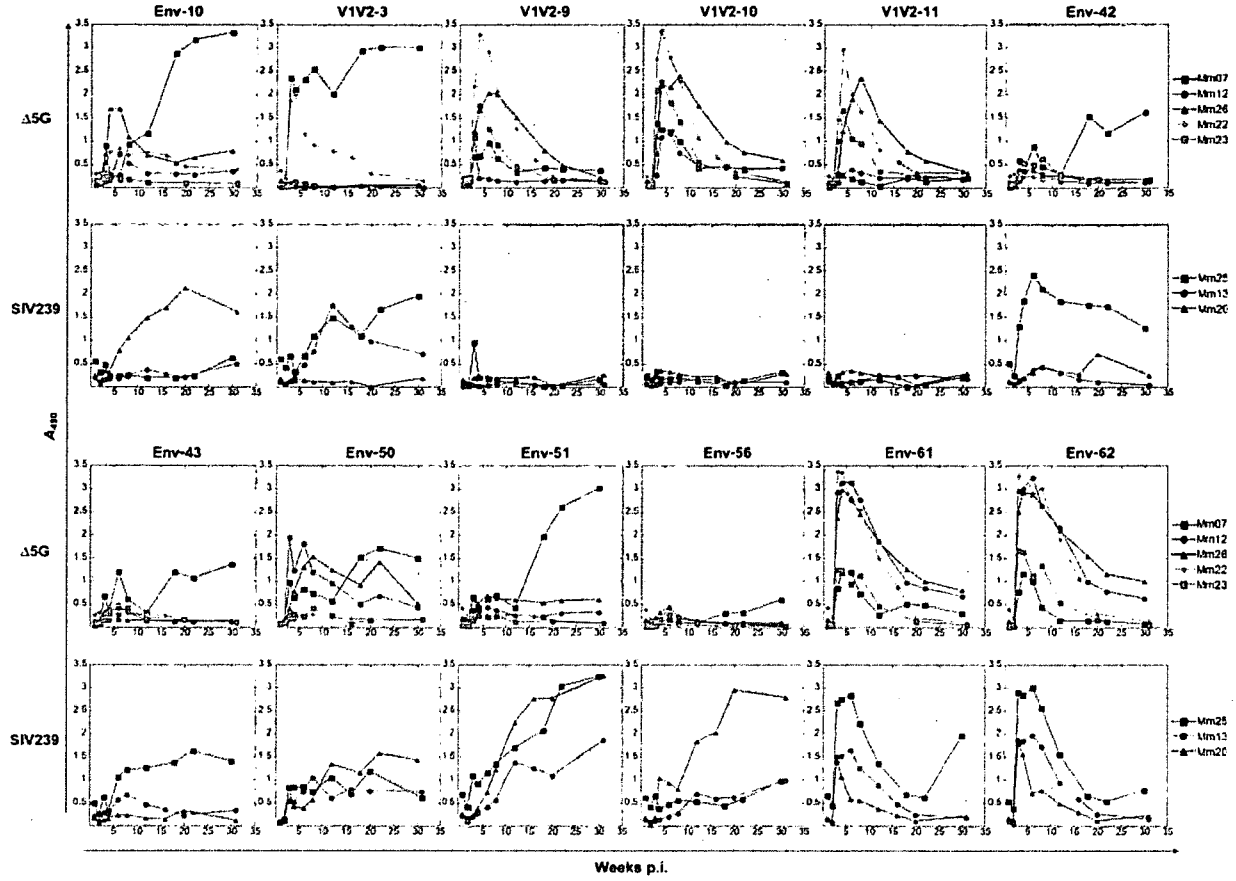


**Fig. 6.** Kinetics of peptide-specific Ab responses in Δ5G-infected and SIV239-infected animals. The kinetics of Ab reaction against peptides selected in the experiments shown in Figs 4 and 5 was determined as $A_{490}$ using plasma diluted 1 : 100 in an ELISA.

Δ5G-specific, as no appreciable capture of SIV239 virion was detected with these samples. Furthermore, this activity was reduced to the level of control IgG (R374) after selective removal of IgG binding to V1V2-9, -10 and -11 peptides, suggesting that virion capture activity is associated with the Δ5G-specific linear epitope Ab (Fig. 7a). By contrast, IgG fractions from SIV239-infected animals collected at 3–4 weeks p.i. did not exhibit appreciable binding activity either to Δ5G virions or SIV239 virions (Fig. 7b). Thus, these results demonstrated that Δ5G infection elicited not only nAb after 8 weeks p.i., but also a much earlier humoral antiviral mechanism in the form of Δ5G-specific virion-binding Ab at 3–4 weeks p.i. in at least two monkeys (Mm07 and Mm22). To examine the relationship between the two antibody activities, we calculated the correlation of virion capture activity of IgG at 3 or 4 weeks p.i. with a peak nAb titre in Δ5G-infected animals (Fig. 2b) and found that this correlation was statistically significant ($r=1$, $P=0.0167$; Fig. 7c).

## DISCUSSION

### nAb response in Δ5G-infected animals

Glycosylation of viral spikes has long been recognized as an effective strategy to evade host (humoral) immune surveillance for several pathogens and for HIV/SIV in particular (Dowling *et al.*, 2007; Fournillier *et al.*, 2001; Haigwood & Stamatatos, 2003; Huso *et al.*, 1988; Reitter *et al.*, 1998). In support of these observations, the data presented here demonstrated that quintuple deglycosylation conferred live attenuated vaccine properties to an SIV239 mutant, Δ5G (Mori *et al.*, 2001); however, a cellular but not humoral response was detected as an immune correlate of the protection of Δ5G-infected animals against SIV239 challenge infection. Therefore, we assumed that the complete control of robust acute virus replication in Δ5G-infected animals beyond the initial cell-mediated control would be due to the development of rapid and effective nAbs. This study indicated that, whereas

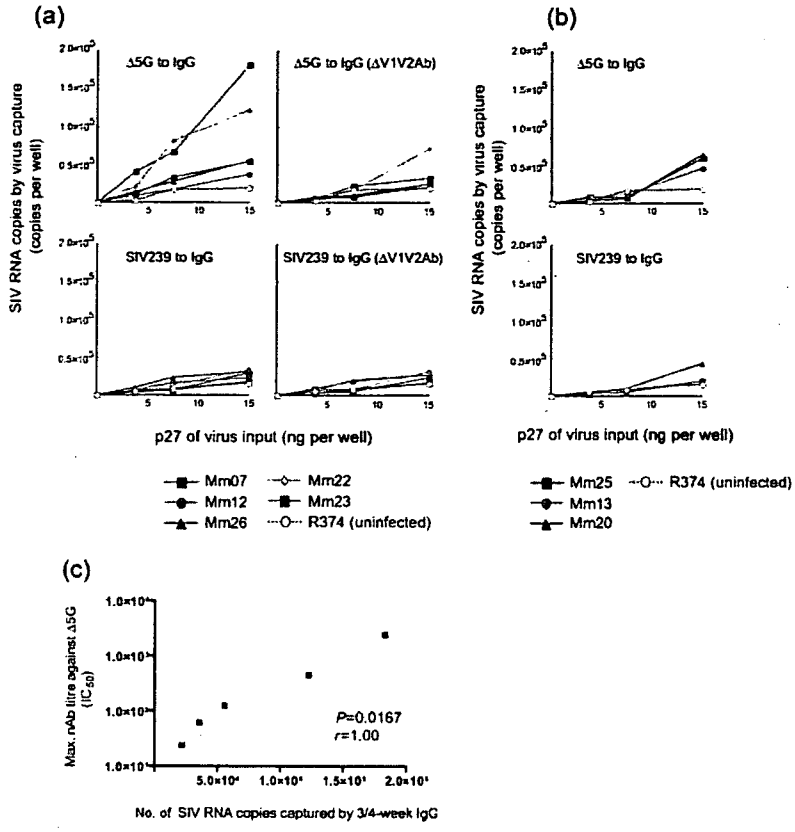


**Fig. 7.** Virion capture activity of IgG from Δ5G-infected and SIV239-infected animals. Virion capture activity of IgG from the plasma of infected animals at 3 or 4 weeks p.i. was determined by increased captured SIV RNA relative to input (3.75, 7.5 and 15 ng $p27^{gag}$) of Δ5G or SIV239. Plasma samples of Δ5G-infected animals (a) and SIV239-infected animals (b) were used for the assay. IgG (ΔV1V2Ab) indicates IgG depleted of Ab binding to V1V2-9, -10 or -11 peptide. R374 was an uninfected monkey. Correlation between virion capture activity at 3 or 4 weeks p.i. and peak nAb titre in Δ5G-infected animals (Fig. 2b) is shown (c).

Δ5G-infected animals clearly exhibited better nAb responses than SIV239-infected animals, the most stringent nAb assay, based on 90% inhibition, provided evidence of nAb titres in only two of five Δ5G-infected animals and the appearance of these titres trailed the decline of acute viral loads by almost 4 weeks (Figs 1 and 2). Therefore, we concluded that, although deglycosylation did promote better development of nAbs in Δ5G-infection than SIV239 infection, it was still too late to control acute viraemia.

Zinkernagel and co-workers have categorized viruses into two types: 'acutely cytopathic viruses' and 'poorly or non-cytopathic viruses' (Hangartner *et al.*, 2006b). The former contains viruses such as vesicular stomatitis virus in mice and influenza virus in humans, whose control depends primarily on a rapid and potent nAb response. The latter comprises viruses such as lymphocytic choriomenigitis virus in mice, and hepatitis B and C viruses and HIV in humans, against which a nAb response is apparent only following the reduction of primary viraemia, and which establish persistent chronic infections. Accordingly, although the viral loads in Δ5G infection resembled 'acutely cytopathic virus' infections, the kinetics of nAbs still conformed to the 'non-cytopathic virus' category. As the difference in nAb response between the two types of virus is determined by their surface glycoproteins (Pinschewer *et al.*, 2004), this study suggests that the deglycosylation of Δ5G could not change this intrinsic property of SIV239.

## Ab responses to Env peptides in Δ5G-infected animals

Aside from nAb, non-nAb responses to linear epitopes in V1/V2 were specifically induced by 3 weeks p.i. in all Δ5G-infected animals (Figs 4, 5 and 6). The heavy glycosylation of viral spikes clearly prevented access of B-cell receptors to the linear Ab epitopes located within limited regions of gp120 in SIV239, and the reduced glycosylation probably promoted better exposure of these linear epitopes in Δ5G (Fig. 4). Accordingly, the Δ5G-specific epitope in V1/V2 should be closely associated with the deglycosylation mutation at aa 171 in gp120 (Fig. 5). We speculate that this Ab induction might contribute to acute viral suppression in Δ5G infection because of the coincident decrease in peak viraemia (Figs 1 and 6). Non-neutralizing Abs can be divided into those that bind to the intact virion surface and debris-specific Ab. The former non-neutralizing Abs have occasional possibilities for antiviral activities such as antibody-dependent cell-mediated cytotoxicity and complement-mediated virus inactivation (Aasa-Chapman *et al.*, 2005; Ahmad & Menezes, 1996; Forthal *et al.*, 2001; Hangartner *et al.*, 2006a). In fact, readily detectable virion

capture Abs were induced in two of five Δ5G-infected animals (Fig. 7, Mm07 and Mm22). The importance of immediate-early suppression of SIV replication for the long-term containment of infection has been demonstrated by studies of post-exposure anti-retroviral therapy (Lifson *et al.*, 2000; Mori *et al.*, 2000). Thus, the early and complete control of viraemia in Δ5G-infected animals clearly suggests an antiviral mechanism(s) acting as early as 2–4 weeks p.i. Therefore, the early detection of IgG capable of virus capture in Δ5G-infected animals may provide mechanisms capable of contributing to undetectable viral load set points (Fig. 1b). The selective generation of such Ab directed to linear Env epitopes is expected.

Interestingly, deglycosylation in gp120 was also associated with a general reduction in the antigenicity of linear epitopes in gp41: the Ab response against the two epitopes that reside in the regions between the two heptad repeats (aa 601–625) and in the C-terminal heptad repeat (aa 660–685), respectively, was markedly reduced (Fig. 4, Table 1). The former corresponds to the highly conserved immunogenic epitope (Benichou *et al.*, 1993; Gnann *et al.*, 1987; Silvera *et al.*, 1994), and the latter corresponds to an epitope identified in the chronic phase of SIVmac251 infection (Silvera *et al.*, 1994) and corresponds to the nAb epitope of HIV-1 known as 2F5 (Muster *et al.*, 1993), although this linear epitope has not been associated with SIV neutralization (Caffrey *et al.*, 1998). Thus, these epitopes are probably exposed on the surface of viral spikes or their degraded fragments in most SIV and HIV-1 isolates with appropriate glycosylation and correct folding. We believe that the loss of glycosylation might induce a slight conformational change in the gp120 protein backbone, resulting in altered interaction of gp120 and gp41. In fact, the region encompassing the former epitope in gp41 was demonstrated to interact with gp120 (Cao *et al.*, 1993; Maerz *et al.*, 2001; York & Nunberg, 2004). As viral spikes determine virus properties such as viral receptor usage and cell tropism (Kolchinsky *et al.*, 2001; Puffer *et al.*, 2002), different cell populations might be infected in Δ5G-infected animals compared with SIV239 infection. More specifically, because of the distinct properties of the virus, vigorous Δ5G replication in the acute phase did not apparently impair immune function and thus established the control of chronic-phase infection and viral replication.

### Host factors required for functional Ab responses against SIV infection

This study also demonstrated remarkable differences in humoral response with regard to nAb and virion capture Ab among Δ5G-infected animals. However, gp120-specific-binding Ab and the linear epitope-specific Ab were initially induced similarly in all animals. These findings imply that Abs measured by ELISA assay and Abs exhibiting antiviral activity are elicited by different pathways and that the properties associated with functional Abs depend largely on the host and underscore the importance of its genetic background. Rhesus macaques are present in various geographical locations within the Asian continent and are subdivided into many subspecies morphologically and genetically (Smith & McDonough, 2005). Some of the genetic differences among rhesus monkeys of different geographical origins, and especially those involving major histocompatibility complex (MHC) genotypes, probably influence the corresponding differences in immune responses, especially cellular response (Bontrop *et al.*, 1996; O'Connor *et al.*, 2003; Reimann *et al.*, 2005). Schmitz *et al.* (2005) reported that Mamu-A*01-positive rhesus monkeys elicited a significantly higher cellular response and lower nAb titres than those in Mamu-A*01-negative animals at the time of challenge infection of animals vaccinated with live attenuated SIV. They suggested that both humoral and cellular immune responses contributed to the protection against the challenge infection and that the relative contribution of each of the responses may be genetically determined. We observed a similar relationship between nAb and cellular responses among Δ5G-infected animals: two animals (Mm07 and Mm22) elicited a lower cellular response while the other three animals (Mm12, Mm23 and Mm26) elicited a higher cellular response (data not shown). Notably two animals exhibiting highly functional Ab (Mm07 and Mm22) were the offspring of seed animals imported from Laos, whilst the others (Mm12, Mm23 and Mm26) were of Burmese origin, suggesting the potential association of such different humoral and cellular responses with host genetic factors. In clinical studies, considerable concordance of adaptive cellular and humoral responses and HIV evolution in monozygotic twins, but not in brothers, infected with the same virus has been reported (Draenert *et al.*, 2006). HIV-1-exposed but uninfected status with significantly higher neutralizing IgA was linked to genotypes on chromosome 22 (Kanari *et al.*, 2005). In the mouse Friend leukemia virus model, MHC II alleles were determined as host genetic factors required for effective nAb response (Miyazawa *et al.*, 1992) and the host genetic factor was mapped to chromosome 15, which was associated with the clearance of viraemia by nAb (Hasenkrug *et al.*, 1995; Kanari *et al.*, 2005).

Taken together, we speculate that the functional humoral response is determined by host genetic properties similar to the cellular immune response. Thus, gaining knowledge of the genetic requirements for both humoral and cellular containment of viral infections will clearly be of primary importance for vaccine development and therapeutics against HIV and other infectious agents.

## NOTE ADDED IN PROOF

A discrepancy in the SIV239-infected animals Mm13 and Mm20 was noted between the result shown in Fig. 2 and that in a previous report Mori *et al.*, 2001. The nAb

response against SIV239 in Mm20 was confirmed at multiple time points in the present study.

## ACKNOWLEDGEMENTS

We thank Kayoko Ueda for excellent technical assistance and Marcelo Kuroda for critical reading of the manuscript. This study was conducted through the Cooperative Research Program in the Tsukuba Primate Research Center, National Institute of Biomedical Innovation, Japan. This work was supported by AIDS research grants from the Health Sciences Research Grants, from the Ministry of Health, Labour and Welfare in Japan, and from the Ministry of Education, Culture, Sports, Science and Technology in Japan.

## REFERENCES

**Aasa-Chapman, M. M., Holuigue, S., Aubin, K., Wong, M., Jones, N. A., Cornforth, D., Pellegrino, P., Newton, P., Williams, I. & other authors (2005).** Detection of antibody-dependent complement-mediated inactivation of both autologous and heterologous virus in primary human immunodeficiency virus type 1 infection. *J Virol* **79**, 2823–2830.

**Ahmad, A. & Menezes, J. (1996).** Antibody-dependent cellular cytotoxicity in HIV infections. *FASEB J* **10**, 258–266.

**Benichou, S., Venet, A., Beyer, C., Tiollais, P. & Madaule, P. (1993).** Characterization of B-cell epitopes in the envelope glycoproteins of simian immunodeficiency virus. *Virology* **194**, 870–874.

**Bontrop, R. E., Otting, N., Niphuis, H., Noort, R., Teeuwsen, V. & Heeney, J. L. (1996).** The role of major histocompatibility complex polymorphisms on SIV infection in rhesus macaques. *Immunol Lett* **51**, 35–38.

**Burns, D. P. & Desrosiers, R. C. (1991).** Selection of genetic variants of simian immunodeficiency virus in persistently infected rhesus monkeys. *J Virol* **65**, 1843–1854.

**Burton, D. R., Desrosiers, R. C., Doms, R. W., Koff, W. C., Kwong, P. D., Moore, J. P., Nabel, G. J., Sodroski, J., Wilson, I. A. & Wyatt, R. T. (2004).** HIV vaccine design and the neutralizing antibody problem. *Nat Immunol* **5**, 233–236.

**Caffrey, M., Cai, M., Kaufman, J., Stahl, S. J., Wingfield, P. T., Covell, D. G., Gronenborn, A. M. & Clore, G. M. (1998).** Three-dimensional solution structure of the 44 kDa ectodomain of SIV gp41. *EMBO J* **17**, 4572–4584.

**Cao, J., Bergeron, L., Helseth, E., Thali, M., Repke, H. & Sodroski, J. (1993).** Effects of amino acid changes in the extracellular domain of the human immunodeficiency virus type 1 gp41 envelope glycoprotein. *J Virol* **67**, 2747–2755.

**Chackerian, B., Rudensey, L. M. & Overbaugh, J. (1997).** Specific *N*-linked and *O*-linked glycosylation modifications in the envelope V1 domain of simian immunodeficiency virus variants that evolve in the host alter recognition by neutralizing antibodies. *J Virol* **71**, 7719–7727.

**Chen, B., Vogan, E. M., Gong, H., Skehel, J. J., Wiley, D. C. & Harrison, S. C. (2005).** Structure of an unliganded simian immunodeficiency virus gp120 core. *Nature* **433**, 834–841.

**Cheng-Mayer, C., Brown, A., Harouse, J., Luciw, P. A. & Mayer, A. J. (1999).** Selection for neutralization resistance of the simian/human immunodeficiency virus $SHIV_{SF33A}$ variant in vivo by virtue of sequence changes in the extracellular envelope glycoprotein that modify *N*-linked glycosylation. *J Virol* **73**, 5294–5300.

**Choi, W. S., Collignon, C., Thiriart, C., Burns, D. P., Stott, E. J., Kent, K. A. & Desrosiers, R. C. (1994).** Effects of natural sequence variation on recognition by monoclonal antibodies neutralize simian immunodeficiency virus infectivity. *J Virol* **68**, 5395–5402.

**Dowling, W., Thompson, E., Badger, C., Mellquist, J. L., Garrison, A. R., Smith, J. M., Paragas, J., Hogan, R. J. & Schmaljohn, C. (2007).** Influences of glycosylation on antigenicity, immunogenicity, and protective efficacy of Ebola virus GP DNA vaccines. *J Virol* **81**, 1821–1837.

**Draenert, R., Allen, T. M., Liu, Y., Wrin, T., Chappey, C., Verrill, C. L., Sirera, G., Eldridge, R. L., Lahaie, M. P. & other authors (2006).** Constraints on HIV-1 evolution and immunodominance revealed in monozygotic adult twins infected with the same virus. *J Exp Med* **203**, 529–539.

**Eberle, J., Loussert-Ajaka, I., Brust, S., Zekeng, L., Hauser, P. H., Kaptue, L., Knapp, S., Damond, F., Saragosti, S. & other authors (1997).** Diversity of the immunodominant epitope of gp41 of HIV-1 subtype O and its validity for antibody detection. *J Virol Methods* **67**, 85–91.

**Forthal, D. N., Landucci, G. & Keenan, B. (2001).** Relationship between antibody-dependent cellular cytotoxicity, plasma HIV type 1 RNA, and $CD4^+$ lymphocyte count. *AIDS Res Hum Retroviruses* **17**, 553–561.

**Fournillier, A., Wychowski, C., Boucreux, D., Baumert, T. F., Meunier, J. C., Jacobs, D., Muguet, S., Depla, E. & Inchauspe, G. (2001).** Induction of hepatitis C virus E1 envelope protein-specific immune response can be enhanced by mutation of *N*-glycosylation sites. *J Virol* **75**, 12088–12097.

**Gnann, J. W., Jr, Nelson, J. A. & Oldstone, M. B. (1987).** Fine mapping of an immunodominant domain in the transmembrane glycoprotein of human immunodeficiency virus. *J Virol* **61**, 2639–2641.

**Haigwood, N. L. & Stamatatos, L. (2003).** Role of neutralizing antibodies in HIV infection. *AIDS* **17** (Suppl. 4), S67–S71.

**Hangartner, L., Zellweger, R. M., Giobbi, M., Weber, J., Eschli, B., McCoy, K. D., Harris, N., Recher, M., Zinkernagel, R. M. & Hengartner, H. (2006a).** Nonneutralizing antibodies binding to the surface glycoprotein of lymphocytic choriomeningitis virus reduce early virus spread. *J Exp Med* **203**, 2033–2042.

**Hangartner, L., Zinkernagel, R. M. & Hengartner, H. (2006b).** Antiviral antibody responses: the two extremes of a wide spectrum. *Nat Rev Immunol* **6**, 231–243.

**Hasenkrug, K. J., Valenzuela, A., Letts, V. A., Nishio, J., Chesebro, B. & Frankel, W. N. (1995).** Chromosome mapping of *Rfv3*, a host resistance gene to Friend murine retrovirus. *J Virol* **69**, 2617–2620.

**Hofmann-Lehmann, R., Swenerton, R. K., Liska, V., Leutenegger, C. M., Lutz, H., McClure, H. M. & Ruprecht, R. M. (2000).** Sensitive and robust one-tube real-time reverse transcriptase-polymerase chain reaction to quantify SIV RNA load: comparison of one- versus two-enzyme systems. *AIDS Res Hum Retroviruses* **16**, 1247–1257.

**Huso, D. L., Narayan, O. & Hart, G. W. (1988).** Sialic acids on the surface of caprine arthritis-encephalitis virus define the biological properties of the virus. *J Virol* **62**, 1974–1980.

**Johnson, W. E., Sanford, H., Schwall, L., Burton, D. R., Parren, P. W., Robinson, J. E. & Desrosiers, R. C. (2003).** Assorted mutations in the envelope gene of simian immunodeficiency virus lead to loss of neutralization resistance against antibodies representing a broad spectrum of specificities. *J Virol* **77**, 9993–10003.

**Kanari, Y., Clerici, M., Abe, H., Kawabata, H., Trabattoni, D., Caputo, S. L., Mazzotta, F., Fujisawa, H., Niwa, A. & other authors (2005).** Genotypes at chromosome 22q12–13 are associated with HIV-1-exposed but uninfected status in Italians. *AIDS* **19**, 1015–1024.

**Kent, K. A., Rud, E., Corcoran, T., Powell, C., Thiriart, C., Collignon, C. & Stott, E. J. (1992).** Identification of two neutralizing and 8 non-neutralizing epitopes on simian immunodeficiency virus envelope

using monoclonal antibodies. *AIDS Res Hum Retroviruses* **8**, 1147–1151.

**Kolchinsky, P., Kiprilov, E., Bartley, P., Rubinstein, R. & Sodroski, J. (2001).** Loss of a single *N*-linked glycan allows CD4-independent human immunodeficiency virus type 1 infection by altering the position of the gp120 V1/V2 variable loops. *J Virol* **75**, 3435–3443.

**Leonard, C. K., Spellman, M. W., Riddle, L., Harris, R. J., Thomas, J. N. & Gregory, T. J. (1990).** Assignment of intrachain disulfide bonds and characterization of potential glycosylation sites of the type 1 recombinant human immunodeficiency virus envelope glycoprotein (gp120) expressed in Chinese hamster ovary cells. *J Biol Chem* **265**, 10373–10382.

**Lifson, J. D., Rossio, J. L., Arnaout, R., Li, L., Parks, T. L., Schneider, D. K., Kiser, R. F., Coalter, V. J., Walsh, G. & other authors (2000).** Containment of simian immunodeficiency virus infection: cellular immune responses and protection from rechallenge following transient postinoculation antiretroviral treatment. *J Virol* **74**, 2584–2593.

**Liu, J., Wang, S., Hoxie, J. A., LaBranche, C. C. & Lu, M. (2002).** Mutations that destabilize the gp41 core are determinants for stabilizing the simian immunodeficiency virus-CPmac envelope glycoprotein complex. *J Biol Chem* **277**, 12891–12900.

**Maerz, A. L., Drummer, H. E., Wilson, K. A. & Poumbourios, P. (2001).** Functional analysis of the disulfide-bonded loop/chain reversal region of human immunodeficiency virus type 1 gp41 reveals a critical role in gp120-gp41 association. *J Virol* **75**, 6635–6644.

**Means, R. E., Greenough, T. & Desrosiers, R. C. (1997).** Neutralization sensitivity of cell culture-passaged simian immunodeficiency virus. *J Virol* **71**, 7895–7902.

**Miyazawa, M., Nishio, J., Wehrly, K. & Chesebro, B. (1992).** Influence of MHC genes on spontaneous recovery from Friend retrovirus-induced leukemia. *J Immunol* **148**, 644–647.

**Mori, K., Yasutomi, Y., Sawada, S., Villinger, F., Sugama, K., Rosenwith, B., Heeney, J. L., Uberla, K., Yamazaki, S. & other authors (2000).** Suppression of acute viremia by short-term postexposure prophylaxis of simian/human immunodeficiency virus SHIV-RT-infected monkeys with a novel reverse transcriptase inhibitor (GW420867) allows for development of potent antiviral immune responses resulting in efficient containment of infection. *J Virol* **74**, 5747–5753.

**Mori, K., Yasutomi, Y., Ohgimoto, S., Nakasone, T., Takamura, S., Shioda, T. & Nagai, Y. (2001).** Quintuple deglycosylation mutant of simian immunodeficiency virus SIVmac239 in rhesus macaques: robust primary replication, tightly contained chronic infection, and elicitation of potent immunity against the parental wild-type strain. *J Virol* **75**, 4023–4028.

**Mori, K., Sugimoto, C., Ohgimoto, S., Nakayama, E. E., Shioda, T., Kusagawa, S., Takebe, Y., Kano, M., Matano, T. & other authors (2005).** Influence of glycosylation on the efficacy of an Env-based vaccine against simian immunodeficiency virus SIVmac239 in a macaque AIDS model. *J Virol* **79**, 10386–10396.

**Muster, T., Steindl, F., Purtscher, M., Trkola, A., Klima, A., Himmler, G., Ruker, F. & Katinger, H. (1993).** A conserved neutralizing epitope on gp41 of human immunodeficiency virus type 1. *J Virol* **67**, 6642–6647.

**Nishimura, Y., Igarashi, T., Haigwood, N., Sadjadpour, R., Plishka, R. J., Buckler-White, A., Shibata, R. & Martin, M. A. (2002).** Determination of a statistically valid neutralization titer in plasma that confers protection against simian-human immunodeficiency virus challenge following passive transfer of high-titered neutralizing antibodies. *J Virol* **76**, 2123–2130.

**Nyambi, P. N., Gorny, M. K., Bastiani, L., van der Groen, G., Williams, C. & Zolla-Pazner, S. (1998).** Mapping of epitopes exposed on intact human immunodeficiency virus type 1 (HIV-1) virions: a new strategy for studying the immunologic relatedness of HIV-1. *J Virol* **72**, 9384–9391.

**O'Connor, D. H., Mothe, B. R., Weinfurter, J. T., Fuenger, S., Rehrauer, W. M., Jing, P., Rudersdorf, R. R., Liebl, M. E., Krebs, K. & other authors (2003).** Major histocompatibility complex class I alleles associated with slow simian immunodeficiency virus disease progression bind epitopes recognized by dominant acute-phase cytotoxic-T-lymphocyte responses. *J Virol* **77**, 9029–9040.

**Ohgimoto, S., Shioda, T., Mori, K., Nakayama, E. E., Hu, H. & Nagai, Y. (1998).** Location-specific, unequal contribution of the *N* glycans in simian immunodeficiency virus gp120 to viral infectivity and removal of multiple glycans without disturbing infectivity. *J Virol* **72**, 8365–8370.

**Pinschewer, D. D., Perez, M., Jeetendra, E., Bachi, T., Horvath, E., Hengartner, H., Whitt, M. A., de la Torre, J. C. & Zinkernagel, R. M. (2004).** Kinetics of protective antibodies are determined by the viral surface antigen. *J Clin Invest* **114**, 988–993.

**Puffer, B. A., Pohlmann, S., Edinger, A. L., Carlin, D., Sanchez, M. D., Reitter, J., Watry, D. D., Fox, H. S., Desrosiers, R. C. & Doms, R. W. (2002).** CD4 independence of simian immunodeficiency virus Envs is associated with macrophage tropism, neutralization sensitivity, and attenuated pathogenicity. *J Virol* **76**, 2595–2605.

**Regier, D. A. & Desrosiers, R. C. (1990).** The complete nucleotide sequence of a pathogenic molecular clone of simian immunodeficiency virus. *AIDS Res Hum Retroviruses* **6**, 1221–1231.

**Reimann, K. A., Parker, R. A., Seaman, M. S., Beaudry, K., Beddall, M., Peterson, L., Williams, K. C., Veazey, R. S., Montefiori, D. C. & other authors (2005).** Pathogenicity of simian-human immunodeficiency virus SHIV-89.6P and SIVmac is attenuated in cynomolgus macaques and associated with early T-lymphocyte responses. *J Virol* **79**, 8878–8885.

**Reitter, J. N., Means, R. E. & Desrosiers, R. C. (1998).** A role for carbohydrates in immune evasion in AIDS. *Nat Med* **4**, 679–684.

**Schmitz, J. E., Johnson, R. P., McClure, H. M., Manson, K. H., Wyand, M. S., Kuroda, M. J., Lifton, M. A., Khunkhun, R. S., McEvers, K. J. & other authors (2005).** Effect of $CD8^+$ lymphocyte depletion on virus containment after simian immunodeficiency virus SIVmac251 challenge of live attenuated SIVmac239Δ3-vaccinated rhesus macaques. *J Virol* **79**, 8131–8141.

**Silvera, P., Flanagan, B., Kent, K., Rud, E., Powell, C., Corcoran, T., Bruck, C., Thiriart, C., Haigwood, N. L. & Stott, E. J. (1994).** Fine analysis of humoral antibody response to envelope glycoprotein of SIV in infected and vaccinated macaques. *AIDS Res Hum Retroviruses* **10**, 1295–1304.

**Smith, D. G. & McDonough, J. (2005).** Mitochondrial DNA variation in Chinese and Indian rhesus macaques (*Macaca mulatta*). *Am J Primatol* **65**, 1–25.

**Wei, X., Decker, J. M., Wang, S., Hui, H., Kappes, J. C., Wu, X., Salazar-Gonzalez, J. F., Salazar, M. G., Kilby, J. M. & other authors (2003).** Antibody neutralization and escape by HIV-1. *Nature* **422**, 307–312.

**Wyatt, R. & Sodroski, J. (1998).** The HIV-1 envelope glycoproteins: fusogens, antigens, and immunogens. *Science* **280**, 1884–1888.

**Wyatt, R., Kwong, P. D., Desjardins, E., Sweet, R. W., Robinson, J., Hendrickson, W. A. & Sodroski, J. G. (1998).** The antigenic structure of the HIV gp120 envelope glycoprotein. *Nature* **393**, 705–711.

**York, J. & Nunberg, J. H. (2004).** Role of hydrophobic residues in the central ectodomain of gp41 in maintaining the association between human immunodeficiency virus type 1 envelope glycoprotein subunits gp120 and gp41. *J Virol* **78**, 4921–4926.

**Yu, D., Shioda, T., Kato, A., Hasan, M. K., Sakai, Y. & Nagai, Y. (1997).** Sendai virus-based expression of HIV-1 gp120: reinforcement by the V(−) version. *Genes Cells* **2**, 457–466.

**Zhang, M., Gaschen, B., Blay, W., Foley, B., Haigwood, N., Kuiken, C. & Korber, B. (2004).** Tracking global patterns of *N*-linked glycosylation site variation in highly variable viral glycoproteins: HIV, SIV, and HCV envelopes and influenza hemagglutinin. *Glycobiology* **14**, 1229–1246.

**Zolla-Pazner, S. (2004).** Identifying epitopes of HIV-1 that induce protective antibodies. *Nat Rev Immunol* **4**, 199–210.

JOURNAL OF VIROLOGY, May 2007, p. 4445–4456 Vol. 81, No. 9
0022-538X/07/$08.00+0 doi:10.1128/JVI.00026-07


# Simian Immunodeficiency Virus (SIV) Infection Influences the Level and Function of Regulatory T Cells in SIV-Infected Rhesus Macaques but Not SIV-Infected Sooty Mangabeys▽

L. E. Pereira,[1] F. Villinger,[1] N. Onlamoon,[1,2] P. Bryan,[1] A. Cardona,[1] K. Pattanapanysat,[2,3] K. Mori,[4]† S. Hagen,[5] L. Picker,[5] and A. A. Ansari[1]*

*Department of Pathology and Lab Medicine, Emory University School of Medicine, Atlanta, Georgia[1]; Department of Immunology, Siriraj Hospital, Mahidol University, Bangkok, Thailand[2]; Thailand Research Fund[3]; Tsukuba Primate Center, NIH, Japan[4]; and Oregon Health and Science University and Oregon National Primate Research Center, Portland, Oregon[5]*

Received 4 January 2007/Accepted 12 February 2007

**Differences in clinical outcome of simian immunodeficiency virus (SIV) infection in disease-resistant African sooty mangabeys (SM) and disease-susceptible Asian rhesus macaques (RM) prompted us to examine the role of regulatory T cells (Tregs) in these two animal models. Results from a cross-sectional study revealed maintenance of the frequency and absolute number of peripheral Tregs in chronically SIV-infected SM while a significant loss occurred in chronically SIV-infected RM compared to uninfected animals. A longitudinal study of experimentally SIV-infected animals revealed a transient increase in the frequency of Tregs from baseline values following acute infection in RM, but no change in the frequency of Tregs occurred in SM during this period. Further examination revealed a strong correlation between plasma viral load (VL) and the level of Tregs in SIV-infected RM but not SM. A correlation was also noted in SIV-infected RM that control VL spontaneously or in response to antiretroviral chemotherapy. In addition, immunofluorescent cell count assays showed that while Treg-depleted peripheral blood mononuclear cells from RM led to a significant enhancement of $CD4^+$ and $CD8^+$ T-cell responses to select pools of SIV peptides, there was no detectable T-cell response to the same pool of SIV peptides in Treg-depleted cells from SIV-infected SM. Our data collectively suggest that while Tregs do appear to play a role in the control of viremia and the magnitude of the SIV-specific immune response in RM, their role in disease resistance in SM remains unclear.**

African primate sooty mangabeys (SM) (*Cercocebus atys*) are a natural host of simian immunodeficiency virus (SIV) but remain asymptomatic throughout the course of infection and do not develop any detectable immunodeficiency or disease. Despite high viremia, naturally or experimentally SIV-infected SM maintain reasonable CD4 T-cell counts and an absence of chronic activation of T cells (10, 33, 39). This symptom-free characteristic of SM is in marked contrast to the CD4 T-cell depletion and disease progression that occur in SIV-infected Asian rhesus macaques (RM) (21, 38). In the latter species, the initial CD8 T-cell-mediated antiviral response generated during the acute phase, although beneficial, proves to be inadequate for viral control and clearance, resulting in chronic viremia and a state of chronic immune activation (24, 34, 38). The increased levels of activation-induced cell death and to various levels bystander apoptosis exhibited by SIV-infected RM are markedly attenuated or absent in SIV-infected SM (38, 39). Since viral loads (VL) in SIV-infected SM reach levels that lead to AIDS in the vast majority of similarly infected RM, the development of disease in the latter species is believed to depend on the quality and/or quantity of the immune response to viral infection rather than VL alone.

While both RM and SM develop readily detectable anti-SIV-specific antibodies following infection, the magnitude of $CD4^+$ and $CD8^+$ SIV-specific cellular immune responses in SIV-infected SM is typically diminished and difficult to detect in comparison to the elevated T-cell SIV-specific immune response in SIV-infected RM (10, 38). It was reasoned that one explanation for the limited virus-specific cellular immune response exhibited by SIV-infected SM could be that this response is secondary to the effect of more-potent and/or a higher level of natural regulatory T cells (Tregs), a cell lineage that has recently been revisited for its role in SIV/human immunodeficiency virus (HIV) pathogenesis. Tregs typically constitute a small percentage of circulating $CD4^+$ T cells (2 to 5% in adult humans) (4, 20, 25, 35). Markers commonly associated with the identification of Tregs include high cell surface levels of the interleukin-2 receptor alpha (IL-2Rα) CD25 and the transcription factor FoxP3 (4, 20, 35, 41, 48). Additional markers include cytotoxic-T-lymphocyte-associated antigen 4, GITR, low levels of the more recently identified Treg marker IL-7 receptor CD127 (26, 27, 37, 43), and, more recently, unique microRNA profiles (9). $CD4^+$ $CD25^{hi}$ Tregs inhibit proliferation of T cells primarily through contact-dependent mechanisms, although cytokine (IL-10 and transforming growth factor β [TGF-β])-mediated inhibition has also been suggested previously (2, 5, 20, 25, 28, 31, 32).

Conflicting data regarding the role of Tregs in lentiviral infection are not uncommon, with some studies suggesting that

* Corresponding author. Mailing address: Department of Pathology and Lab Medicine, Emory University School of Medicine, 101 Woodruff Circle, Rm. 2309, Atlanta, GA 30329. Phone: (404) 712-2834. Fax: (404) 712-1771. E-mail: pathaaa@emory.edu.

† Present address: AIDS Research Center, National Institute of Infectious Disease, Tokyo, Japan.

▽ Published ahead of print on 21 February 2007.

the level of Tregs is unaffected by infection and others showing either an expansion or a decline in Tregs in SIV/HIV-infected hosts (1, 3, 12, 22, 29, 30, 45, 47). This apparent disparity is in part due to differences in the chosen marker(s) for Treg identification, the lack of optimized techniques utilized for Treg quantification (cellular gene expression versus flow cytometry) and data analysis (frequency versus absolute numbers [ABS]), and the stage of infection at the time of sampling. To gain a better understanding of Treg dynamics in SIV pathogenesis, we performed a comprehensive study involving the phenotypic analysis of Tregs from peripheral blood mononuclear cells (PBMCs) from uninfected and SIV-infected SM and RM during the acute, early chronic, and late chronic stages of infection. The effect of antiretroviral therapy (ART) on Treg levels in SIVmac-infected RM was also determined. In addition, a characterization of Treg function in SIV-infected RM and SM was performed. The basic aim of this study is twofold: first, to determine the relationship, if any, between SIV infection and the level and/or function of Tregs in RM and SM, and second, to determine if this cell lineage plays a role in the SIV-specific adaptive immune response and/or generalized immune activation that is muted in SIV-infected SM but readily exhibited by SIV-infected RM. Our results suggest a decline in the number of Tregs in SIV-infected RM and a correlation between Tregs and levels of VL and controlled immune activation in this species. However, the frequency and ABS of Tregs alone cannot account for either VL or disease resistance in the SIV-infected SM.

## MATERIALS AND METHODS

**Animals and infections.** The healthy uninfected and the SIV-infected RM and SM were housed at Yerkes Regional Primate Research Center (YRPRC) of Emory University or at the Oregon National Primate Research Center (ONPRC) at the University of Oregon. Their housing, care, diet, and maintenance conformed to the guidelines of the Committee on the Care and Use of Laboratory Animals of the Institute of Laboratory Animal Resources, National Research Council, and the Health and Human Services guidelines *Guide for the Care and Use of Laboratory Animals* (28a). The sources of the samples from the SIV-infected animals were as follows.

(I) SM. The SIV-noninfected SM and SM that were naturally infected were of comparable ages and were part of breeding colonies maintained at the YRPRC field station. A group of SIV-negative SM were experimentally infected with SIV (a viral stock of an isolate from a mangabey, FUo, that readily infects and replicates in SM monkeys; courtesy of S. Staprans, Emory University) and were housed in individual cages at the main station of the YRPRC. These monkeys served as a source for the longitudinal SM study.

(II) RM. RM involved in the longitudinal study consisted of two groups of animals: one group was infected intravenously with 200 50% tissue culture infective doses of SIVmac239, and the other was infected with 10,000 50% tissue culture infective doses. A subset of the latter group of SIVmac239-infected RM were treated with PMPA (9-(2-phosphonomethoxypropyl)adenine) (20 mg/kg of body weight subcutaneously daily for 28 days after reaching the VL set point) and were utilized to study the effects of antiviral therapy on Tregs. All uninfected and SIV-infected RM used in the study were of comparable ages.

**Specimen collection.** PBMCs were isolated by standard Ficoll-Hypaque gradient centrifugation from whole blood. White blood cell, platelet, and total lymphocyte counts were determined using standard methods and used to calculate absolute values. Lymph nodes and various tissues were obtained at necropsy from five uninfected RM and four SIVmac239-infected RM that were sacrificed due to end-stage AIDS. Single-cell suspensions of lymph node cells were obtained by teasing the cells out of the respective nodes. Mucosal intraepithelial and lamina propria lymphocytes were obtained after serial incubation in EDTA, digestion with collagenase (Worthington type IV), and purification/enrichment on discontinuous 30/60% Percoll gradients.

**Flow cytometry analysis.** Multiple monoclonal antibodies (MAb) with specificity for human CD4, CD25, FoxP3, GITR, and CD127 were first screened in multiple combinations with a variety of fixing conditions to identify those that provided optimal data (similar to human Tregs) for the identification of RM and SM Tregs. From the list of clones screened, the following antibody clones were selected for the immunophenotyping studies of Tregs reported herein: CD4-peridinin chlorophyll protein (clone L200), CD127-phycoerythrin (PE), CD95-fluorescein isothiocyanate (FITC) (clone DX-2) (all purchased from BD Pharmingen, San Diego, CA), CD25-PE (clone 4E3; Miltenyi Biotec, Auburn, CA), and FoxP3-allophycocyanin (clone PCH101 or 236A/E7; E-Bioscience, San Diego, CA). Cells were first incubated with 1 μg/ml of anti-FcR antibody (clone 2.4G2; courtesy of R. Mittler, Emory University) for 15 min at 4°C, washed, and then surface stained for 15 min at 4°C with predetermined optimal concentrations of CD4-peridinin chlorophyll protein, CD95-FITC, and CD25-PE or CD127-PE. Fixation and intracellular staining to detect FoxP3 were performed according to an E-Biosciences protocol. Appropriate MAb isotype controls were included. The study of cell activation markers included the use of MAb against CD25 (Miltenyi Biotec), CD69 (clone FN50; BD Pharmingen), and HLA-DR (clone L243; BD Pharmingen). Flow cytometric acquisition of at least 100,000 events from each sample was performed on a FACSCalibur flow cytometer. Samples were also analyzed on an LSR II system by use of the following panel: CD4-AmCyan (L200) and CD95-PECy7 (DX2), both from BD Biosciences; CD25-biotin (4E3; Miltenyi); streptavidin-ECD (Beckman-Coulter, Miami, FL); and FoxP3-PE (206D; BioLegend, San Diego, CA). Data acquisition and analysis were done using CellQuest (BD Biosciences) and FlowJo (TreeStar, Ashland, OR) software, respectively. Data reported herein represent results acquired utilizing the FACSCalibur system.

**Cell isolation and in vitro suppression/MLR assays.** $CD4^+$ T cells were isolated from PBMCs by negative selection using an RM CD4 T-cell enrichment kit (StemCell Technologies, Inc.). Enriched cells were stained with CD25-PE (5 μl/million cells) for 15 min at 4°C. $CD4^+$ $CD25^+$ Treg cells were purified using an anti-PE EasySep kit (StemCell Technologies, Inc.). Flow cytometry was performed on aliquots to confirm the phenotype of the isolated responder cells ($CD4^+$ $CD25^-$) and that of Tregs ($CD4^+$ $CD25^+$). In vitro mixed lymphocyte reaction (MLR) assays were performed to assess Treg function. Briefly, highly enriched populations of responder $CD4^+$ T cells depleted of $CD25^+$ T cells were incubated in triplicate with a fixed number of a pool of allogeneic irradiated stimulator cells in a 96-well plate in the absence and presence of graded numbers of $CD4^+$ $CD25^{hi}$ cells (autologous to the responder cells). The cultures were incubated for 5 days at 37°C and 5% $CO_2$. Sixteen hours prior to harvest, cells were pulsed with 1 μCi/well $^3$[H]thymidine. Cultures were harvested and the mean uptake of $^3$[H]thymidine determined using standard scintillation counting. One unit of Treg function was defined as the number of Tregs that inhibited the *allo*-MLR by 1/3. In addition, an *allo*-MLR precursor frequency was determined, using highly enriched $CD4^+$ T cells with and without depletion of the $CD4^+$ $CD25^+$ T cells. Various numbers of these responder cells were cocultured with a fixed number of an irradiated mixed pool of stimulator cells, with each dilution cocultured in 24 replicate wells. The number of wells showing significant proliferation was defined as individual wells showing uptake of $^3$[H]thymidine, which was 3 standard deviations (SD) above the mean value of the appropriate number of responder cells cultured alone. The *allo*-reactive precursor frequencies were estimated based on the "single hit" Poisson model as described by Strijbosch et al. (40), who kindly supplied us with software for the analyses performed herein.

**Determination of SIV antigen-specific $CD4^+$ and $CD8^+$ responses.** Aliquots of unfractionated or $CD4^+$/$CD25^+$-depleted PBMCs from each monkey were cultured for 2 h with eight individual pools of overlapping SIV Env peptides (25-mers overlapping by 13) or eight individual pools of overlapping Gag peptides (20-mers overlapping by 12) covering the entire SIV env and gag region (based on the SIVmac239 sequence), followed by the addition of brefeldin A and incubation overnight. Cells were then washed and surface stained for CD4 and CD8 (CD8-FITC; BD Pharmingen) and then fixed/permeabilized and stained for intracellular gamma interferon (IFN-γ) (allophycocyanin conjugated; BD Pharmingen). The frequency of IFN-γ-producing $CD4^+$ or $CD8^+$ cells was determined by standard flow cytometric analysis.

**Determination of VL.** Plasma VL were determined by the Virology Core of the Emory University CFAR by use of a competitive reverse transcriptase PCR assay.

**Statistical analysis.** Data are represented as means ± SD and were analyzed by using the two-tailed Student *t* test. A linear least-square regression model and the Mann-Whitney test (two tailed) were used to derive a correlation between VL and Tregs. A $P$ value of $<0.05$ was considered to be statistically significant.

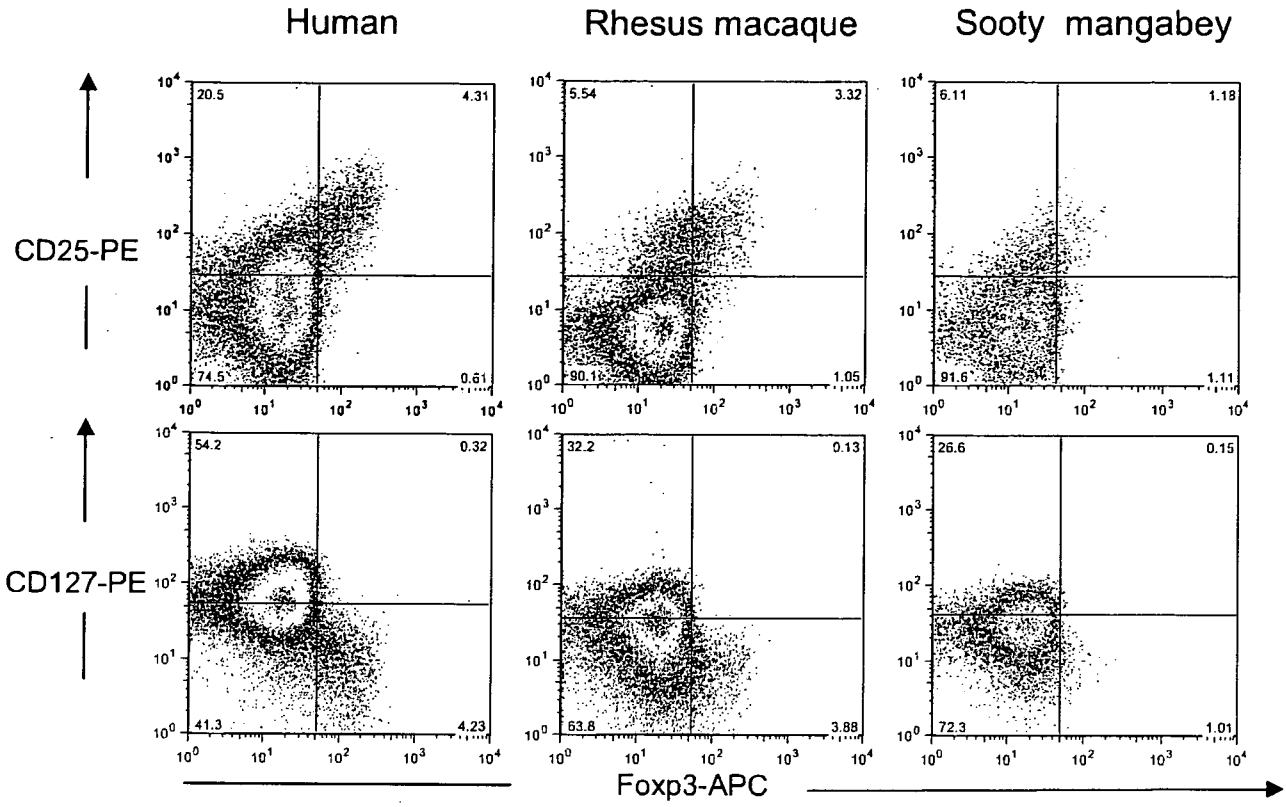


FIG. 1. Expression of FoxP3 on CD4$^+$ T cells from humans and the nonhuman primates RM and SM. PBMCs from uninfected human volunteers, RM, and SM were stained for cell surface expression of CD4 and CD25 or CD127. The stained cells were fixed and stained intracellularly with anti-FoxP3. Shown are representative profiles for each species. The number in each quadrant indicates the frequency of gated CD4$^+$ T cells that express the relevant marker. APC, allophycocyanin.

## RESULTS

**Expression of CD127$^{lo}$ or CD25$^{hi}$ in combination with FoxP3 enables Treg identification in both SM and RM.** Recent studies have demonstrated that the cell surface expression of CD127$^{lo}$ in combination with CD25$^+$ or in combination with FoxP3 can be used to accurately identify Treg subsets in human peripheral blood (26, 37). To determine if a similar method can be applied to nonhuman primates, PBMCs were isolated from uninfected SM ($n$ = 12) and RM ($n$ = 12), and the CD25$^{hi}$ FoxP3$^+$ or CD127$^{lo}$ FoxP3$^+$ population within the total CD4$^+$ T-cell population was measured. PBMCs from healthy adult human volunteers ($n$ = 3) were also analyzed for comparison. As indicated by the representative flow cytometric profiles in Fig. 1, the frequency of CD4$^+$ CD25$^{hi}$ FoxP3$^+$ cells was similar to that of the CD4$^+$ CD127$^{lo}$ FoxP3$^+$ subset for each species. On average, the percentage of CD4$^+$ CD25$^{hi}$ FoxP3$^+$ cells was lower in RM (3.0% ± 0.59%) than in humans (4.33% ± 0.15%), and SM expressed the lowest frequency of Tregs (1.9% ± 0.47%). This difference in cell frequency was reflected in the ABS of Tregs, with RM possessing about a twofold-greater level of Tregs than SM (Table 1). This apparent species-specific difference may be secondary to various levels of cross-reactivity with the FoxP3 MAb, although staining with two additional FoxP3-specific MAb clones generated similar results. There was no significant difference in mean density of FoxP3 expression in RM and SM (data not shown). Thus, it appears that the conventional Treg markers CD25$^{hi}$ and FoxP3 can be utilized to identify Tregs in RM and even SM, in agreement with a recent study (42), and the data are also supported by the results obtained by functional assays, such as

TABLE 1. Frequencies and ABS of Tregs within the total CD4$^+$ T-cell population and the memory and naïve CD4$^+$ T-cell subsets in uninfected (SIV$^-$) and SIV-infected (SIV$^+$) RM and SM from a cross-sectional study[a]

| CD4$^+$ population | Primate species and SIV infection status | Frequency of Tregs | ABS of Tregs/μl blood |
|---|---|---|---|
| Total | SIV$^-$ SM | 1.9 ± 0.47 | 28 ± 13 |
| | SIV$^+$ SM | 1.66 ± 0.45 | 18 ± 7 |
| | SIV$^-$ RM | 3 ± 0.59 | 66 ± 16 |
| | SIV$^+$ RM | 2.88 ± 0.77 | 33 ± 19 |
| Memory (CD95$^+$) subset | SIV$^-$ SM | 3.66 ± 1.41 | 19 ± 10 |
| | SIV$^+$ SM | 2.08 ± 0.89 | 17 ± 8 |
| | SIV$^-$ RM | 4.76 ± 1.02 | 41 ± 14 |
| | SIV$^+$ RM | 4.24 ± 1.2 | 24 ± 14 |
| Naïve (CD95$^-$) subset | SIV$^-$ SM | 1.51 ± 0.98 | 12 ± 8 |
| | SIV$^+$ SM | 1.24 ± 1.25 | 2 ± 0.7 |
| | SIV$^-$ RM | 1.77 ± 0.5 | 25 ± 10 |
| | SIV$^+$ RM | 1.1 ± 0.56 | 8 ± 6 |

[a] PBMCs from 12 SIV$^-$ and 12 SIV$^+$ animals of each of the two primate species RM and SM were analyzed.

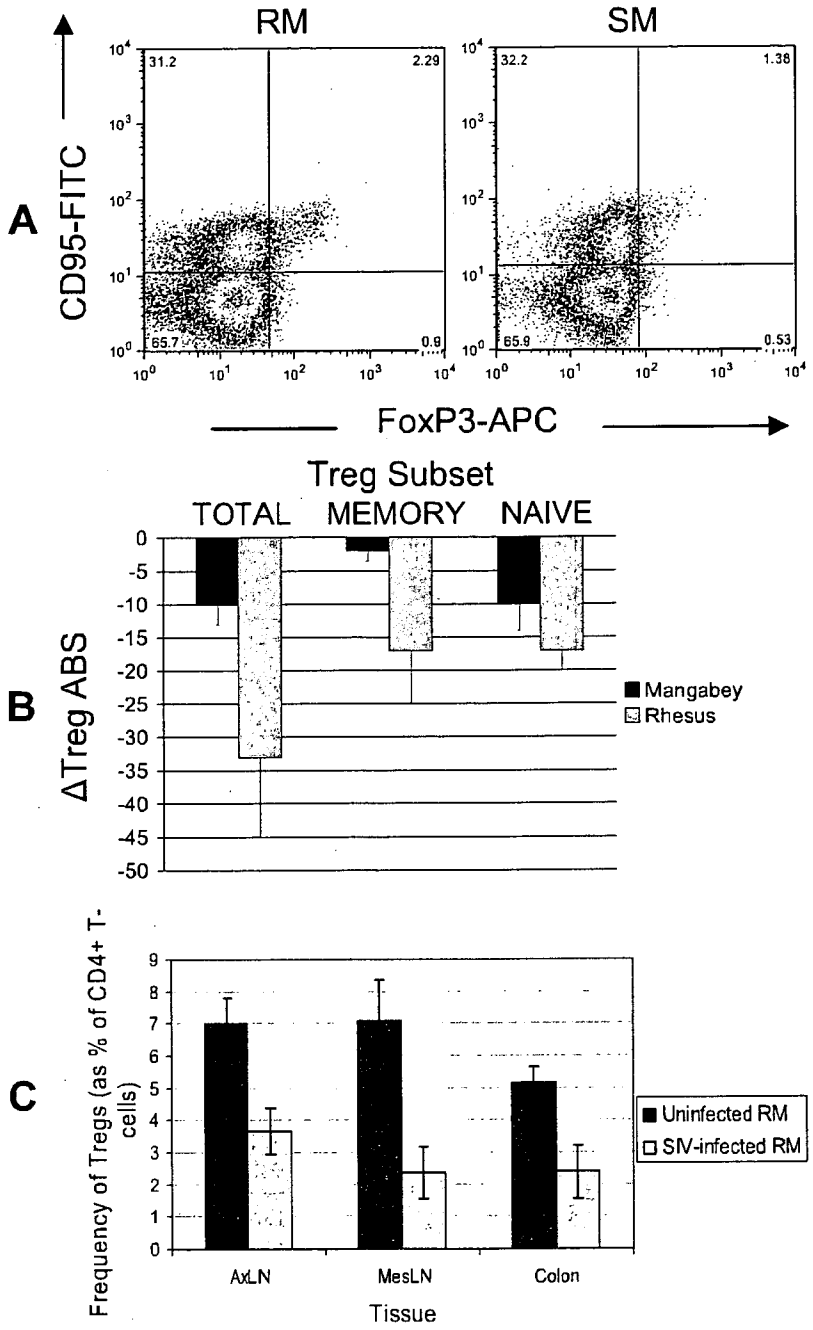


FIG. 2. Cross-sectional study of Treg levels in chronically SIV-infected SM and RM. (A) Representative flow cytometric profile illustrating the FoxP3$^+$ populations within memory (CD95$^+$) and naïve (CD95$^-$) CD4$^+$ subsets in RM ($n$ = 12) and SM ($n$ = 12). (B) Data obtained for uninfected monkeys were used to determine the change in ABS for each Treg subset in SIV-infected SM and RM. (C) The frequencies of Tregs (means ± SD) in the axillary lymph nodes (AxLN), mesenteric lymph nodes (MesLN), and colon were determined for uninfected ($n$ = 5) and SIV-infected ($n$ = 4) RM.

the in vitro suppression/MLR assays utilizing the CD4$^+$ CD25$^+$ subset (see below).

**The ABS of peripheral Tregs decrease significantly in RM but not SM following SIV infection.** To determine if the distinct clinical course and immune responses exhibited by SIV-infected RM and SM are due to differences in the levels of Tregs, a cross-sectional study was performed. PBMCs from 12 individual SIVmac239 chronically infected RM with relatively high VL (>100,000 copies of viral RNA [vRNA]/ml of plasma) and 12 naturally chronically SIV-infected (FUo viral isolate) SM with similar VL were analyzed for frequencies and ABS of Tregs. The frequencies of Tregs within the total CD4$^+$ popu-

lation and the $CD4^+$ memory and naïve subsets were determined. The cell surface marker CD95 was used to distinguish between memory ($CD95^+$) and naïve ($CD95^-$) subsets in RM and SM, as previously described (6, 42), and results are illustrated in Fig. 2A. Since CD4 T-cell levels changed dramatically over the course of infection, particularly in RM, it was reasoned that the data on frequency alone may not be an accurate reflection of true physiological changes. Therefore, the mean ABS of Tregs within each $CD4^+$ subset was also calculated; these data are summarized in Table 1. A feature common to both species is that the predominant frequency and ABS of Tregs appear in the memory $CD4^+$ T-cell subset (Table 1 and Fig. 2A). Conversely, if considering the total $CD25^{hi}$ $FoxP3^+$ Treg fraction, memory and naïve subsets are still distinguishable (flow cytometric profile not shown), with the majority of Tregs possessing a memory phenotype. The frequencies of $CD95^+$ $CD25^{hi}$ $FoxP3^+$ Tregs would typically range from 60 to 70% in both uninfected RM and SM (Table 1). The examination of $CD127^{lo}$ $FoxP3^+$ subsets revealed similar results (not shown).

A comparative analysis of the frequencies of Tregs in uninfected versus chronically infected animals showed a minor decline in frequency of Tregs in the total population and the naïve and memory subsets in both RM and SM. However, the analysis of ABS revealed a notable change in the level of Tregs exhibited by the chronically SIV-infected animals. As indicated in Fig. 2B, SIV-infected SM exhibited a minimal change in total Treg ABS ($P = 0.10$) while a clear significant decrease was observed in chronically SIV-infected RM ($P = 0.00026$). Although a decrease in the naïve Treg subset was observed in SIV-infected SM, normal levels of memory Treg levels were maintained. However, in SIV-infected RM the naïve and memory Treg subsets were threefold and twofold lower, respectively, than the levels in healthy uninfected RM. The decrease in ABS but not the frequency of Tregs in SIV-infected RM suggests that the decrease is not specific to the Treg subset but likely reflects the overall depletion of $CD4^+$ T cells that occurs over the course of SIV infection. A limited study of the frequencies of Tregs in the axillary lymph nodes, mesenteric lymph nodes, and colons from five uninfected and three SIVmac239-infected RM (obtained during autopsy) indicated that, following SIV infection, a decrease in Tregs also occurs in these major sites of infection, at least during the terminal stages of the disease (Fig. 2C). Additional testing of samples from other organs, such as the spleen and liver, and bronchoalveolar lavage specimens did not reveal any noticeable difference (data not shown). Thus, while the frequencies of peripheral Tregs remained relatively unchanged in both chronically SIV-infected SM and RM, these values masked the substantial decrease that occurred in the ABS of Tregs in SIV-infected RM and the maintenance of such cells in SIV-infected SM. Since the regulatory effect of Tregs depends largely on their ratio to memory T cells, this factor was also considered for uninfected and SIV-infected RM and SM. Results suggest a slight decrease in total Treg:memory $CD4^+$ T-cell ratio in SIV-infected RM ($0.081 \pm 0.029$ to $0.06 \pm 0.018$; $P = 0.061$), while the decrease in the ratio in SIV-infected SM appeared to be statistically significant ($0.056 \pm 0.025$ to $0.021 \pm 0.012$; $P = 0.038$). However, it is unclear if these are accurate representations of true cellular ratios, given the immense variability in the numbers of CD4 T cells following infection, particularly in the SM that were sampled.

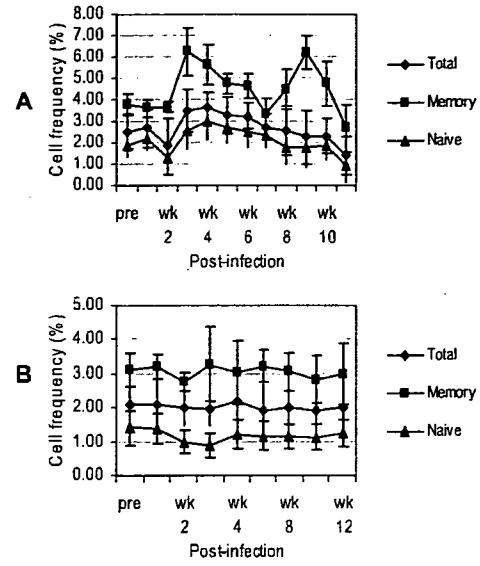


FIG. 3. Longitudinal study of Tregs during the acute phase of SIV infection in RM and SM. A total of 26 RM and three SM were experimentally infected intravenously with SIVmac239 and SM SIV isolate FUo, respectively, and the mean frequencies (±SD) of Tregs within the total $CD4^+$ population and within the memory and naïve $CD4^+$ T-cell subsets were determined by flow cytometry at the indicated time points from preinfection (pre) to 12 weeks (wk) p.i.

**SIV-infected RM but not SIV-infected SM exhibit an increased Treg response during the acute phase of infection.** Since there was a marked decrease in the ABS of Tregs in SIV-infected RM during the chronic-viremia period, it was important to determine the kinetics by which such a decrease occurs in this species and whether any changes could be observed during the same acute-infection period in SM. A longitudinal study was performed in which a total of 26 RM and, for comparison, three SM were monitored prior to and at weekly time intervals during the acute viremia phase following experimental infection with SIVmac239 or FUo viral isolates, respectively. Both species exhibited a peak in VL ($>10^6$ copies/ml) at ~2 weeks postinfection (p.i.), and the VL remained at or near this level ($10^4$ to $10^6$ copies/ml) over the next 10 weeks of SIV infection (not shown). Figure 3A and B show the mean frequencies of total Tregs within the $CD4^+$ T-cell population and the mean frequencies of naïve and memory $CD4^+$ T cells that express the Treg phenotype in PBMC samples from SIV-infected RM and SM. As shown, the SIVmac239-infected RM showed a slight decrease in the frequency of total Tregs within the first 2 weeks of infection, reflecting the rapid decline in total CD4 T cells during this period of infection. This decline was followed by an ~2-fold increase in the frequency of Tregs at 3 weeks p.i., particularly within the memory subset; however, this sharp rise was not reflected by an increase in ABS, suggesting that a depletion of memory CD4 T cells other than Tregs contributed to this observation. Indeed, there was a larger decline in memory $CD4^+$ T cells (not shown), resulting in an overall doubling in the ratio of Tregs:$CD4^+$ T cells. Similarly, there appeared to be another increase in the fre-

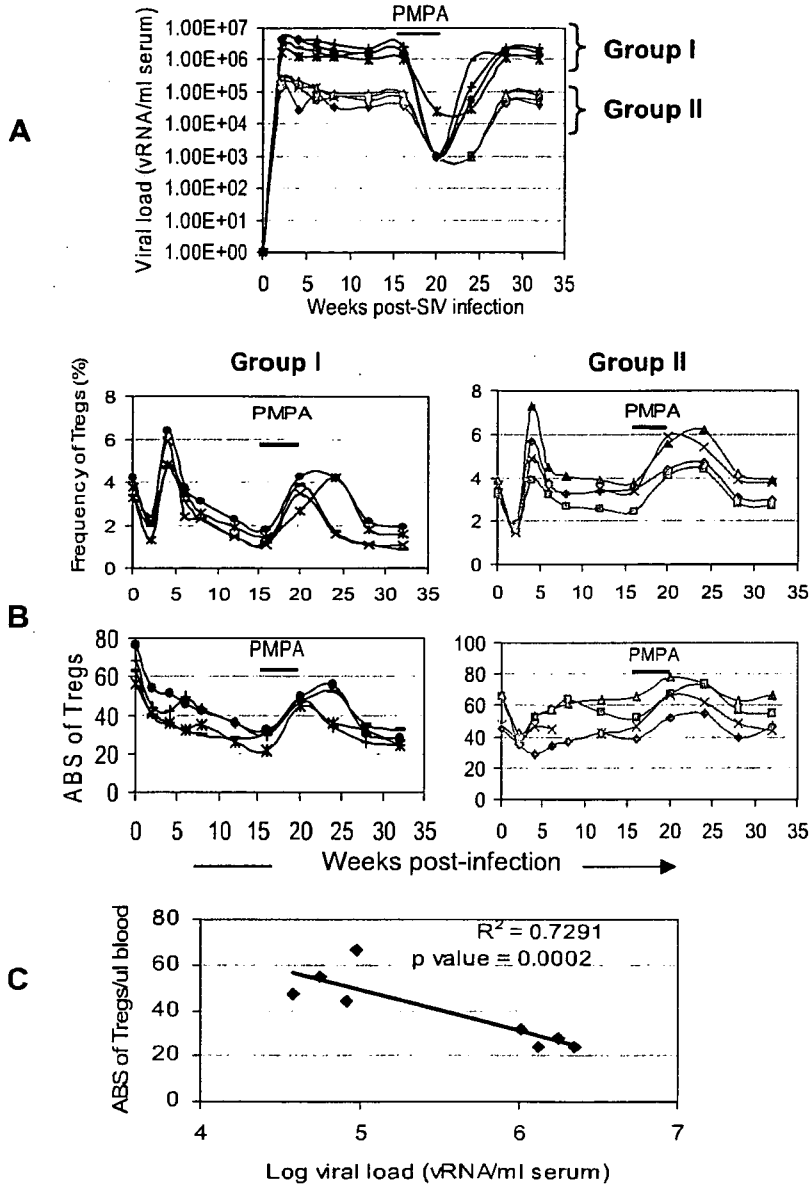


FIG. 4. Longitudinal study of the levels of peripheral Tregs during acute and chronic SIV infection in RM. A total of 26 RM were experimentally infected intravenously with SIVmac239. (A) Plasma VL and (B) frequencies and ABS of Tregs were determined over the course of infection. Data shown are for eight such animals, four with high VL and four with low VL. This group of animals was administered the nucleoside reverse transcriptase inhibitor PMPA at ~16 weeks p.i. (20 mg/kg daily for 30 days). (C) The correlation between VL and ABS of Tregs during the chronic phase was determined.

quency of Tregs within the memory $CD4^+$ subset at 9 weeks p.i., followed by a sharp decline in all Treg subsets. The frequency (Fig. 3B) and ABS (not shown) of Tregs in SIV-infected SM, on the other hand, remained generally unaltered during the first 12 weeks of infection.

**Plasma VL and immune activation inversely correlate with the level of circulating Tregs in SIV-infected RM but not SIV-infected SM.** The longitudinal analysis of Tregs in SIVmac239-infected RM following the acute phase revealed a recovery in the level of Tregs in a few of the animals, and a closer examination of these observations suggested that this resurgence in Tregs was related to a lower VL (Fig. 4). This finding prompted us to examine the data on the frequency and ABS of Tregs as a function of VL. The data were divided into two groups of SIV-infected RM, with one group exhibiting relatively high VL set points ($>10^5$ vRNA/ml serum) (group I) and the other displaying low VL set points ($<10^5$ vRNA/ml serum) (group II). Whereas similar trends were observed in both groups during the first 4 weeks of infection, a progressive decrease in the frequency and ABS of Tregs was observed for group I (high VL) while the ABS of Tregs in group II (low VL) began to recover after 4 weeks, with frequencies remaining

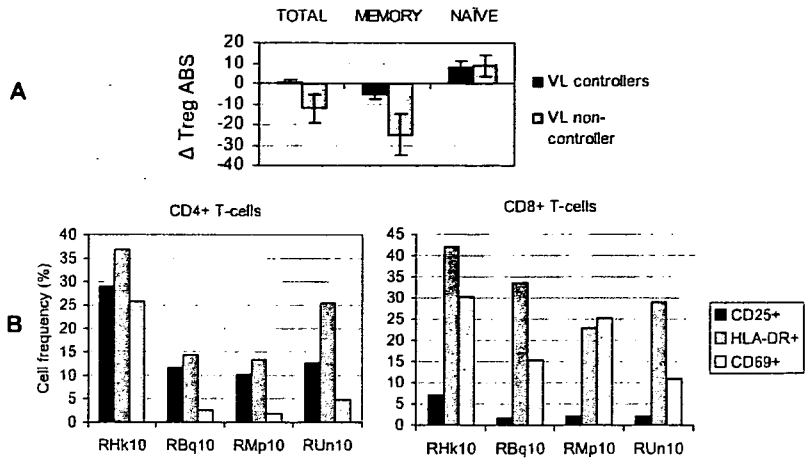


FIG. 5. Analysis of Treg levels and frequencies of activated cells in PBMCs from chronically SIV-infected RM (group III, $n = 3$) that spontaneously control VL in the absence of ART. Shown for comparison are data for PBMCs from monkey RHk10, an untreated SIV-infected RM with high VL. (A) The change in ABS of each Treg subset was determined ~8 months after experimental infection with SIVmac239. Means ± SD are shown. (B) The frequencies of $CD4^+$ and $CD8^+$ T cells expressing the activation markers CD25, CD69, and HLA-DR were determined. The RM with high VL is RHk10.

near baseline. Analysis by the linear-regression method and the Mann-Whitney test revealed a significant inverse correlation between the VL and ABS of Tregs during the chronic phase of infection (Fig. 4C) ($r^2 = 0.730$, $P = 0.0002$). In contrast, a similar comparison between VL and Tregs in 12 SIV-infected SM with low viremia and nine SIV-infected SM with high viremia revealed no correlation (data not shown).

As expected, treatment of both groups of RM with the nucleoside reverse transcriptase inhibitor PMPA (20 mg/kg) daily for 4 weeks resulted in a decline in viremia; an accompanying increase in the frequency and ABS of Tregs was also observed. This increase in Tregs was once again reflective of total CD4 T-cell levels. However, the VL in group I soon increased to high set point levels even before the completion of treatment, leading to a continued decline in the level of Tregs, while group II exhibited an increase in the frequency and ABS of Tregs that was maintained even after viremia returned to a lower set point. Analysis of Tregs in another group (group III) of three chronically SIV-infected RM (RBq10, RMp10, and RUn10) that spontaneously maintained low VL (less than $10^3$ vRNA/ml serum) in the absence of ART revealed similar results (Fig. 5). Shown for comparison are results for the SIV-infected RM RHk10, which is representative of VL noncontrollers ($n = 3$) that were not provided ART. Data for this particular animal are shown since it was infected at the same time with the same inoculum as the other three VL controllers included in this experiment. Analysis of Tregs in PBMC samples from these RM prior to and approximately 32 weeks after SIV infection revealed that the loss of Tregs in VL noncontroller animals ($\Delta ABS = -25$) was significantly greater ($P < 0.05$) than that in the VL controllers ($\Delta ABS = -5$), with a particularly pronounced decline in the memory Treg subset (Fig. 5A). To determine if there was a correlation between this marked difference in Tregs and the state of immune activation, the expression levels of the activation markers CD25, CD69, and HLA-DR on $CD4^+$ and $CD8^+$ T cells were assessed. Indeed, the frequencies of activated $CD4^+$ and $CD8^+$ T cells in VL controllers were on average significantly lower than levels in the noncontrollers (Fig. 5B). These data indicate that recovery and/or maintenance of Tregs was associated with low plasma VL and low immune activation in chronically SIV-infected RM.

**Treg function is maintained in chronically SIV-infected RM and SM.** Although determining the frequency and VL of Tregs during SIV infection sheds some light on their role in SIV pathogenesis, it is equally important to assess the effect on SIV infection on Treg function. Tregs are characterized by their ability to suppress the activation and effector function of T cells predominantly by a contact-dependent mechanism (28, 32). To compare the inhibitory functions of Tregs in uninfected and SIV-infected SM and RM, two different assays were performed. In the first assay, CD25-depleted $CD4^+$ responder T cells from uninfected RM ($n = 9$) and SM ($n = 9$) were cocultured with a mixed pool of irradiated allogeneic PBMCs from RM and SM, respectively, in the absence (control) or presence of 1:1, 0.5:1, 0.25:1, and 0.125:1 autologous Tregs: CD25-depleted $CD4^+$ T cells. As seen in the representative profiles in Fig. 6A, Tregs from each of the two species appeared to decrease the *allo*-proliferative response. In efforts to determine whether there were differences in Treg activity, relative units of Tregs were calculated from such data. Thus, the number of Tregs that decreased the proliferative response by 33.3% was defined as 1 U of activity, which was then multiplied to derive the units of activity per million Tregs. The calculated Treg units of activity from one such data set were 9, 12, and 20 per million Tregs in three RM and 21, 31, and 38 per million Tregs in three SM and are representative of the three independent assays performed. These data suggest that there is perhaps increased functional Treg activity in uninfected SM compared to activity in uninfected RM; however, to confirm this observation an additional functional assay to further compare Tregs from uninfected and SIV-infected animals from the two species was performed. A limiting dilution assay was thus set up in which a fixed number of irradiated stimulators

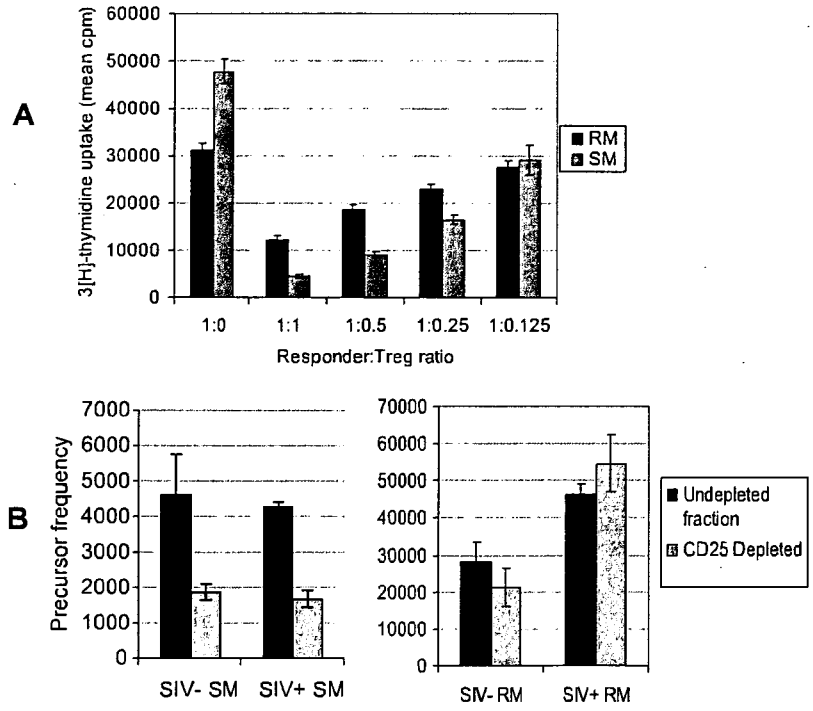


FIG. 6. In vitro MLR assay to demonstrate the effect of Tregs on cell proliferation in uninfected RM and SM. (A) Treg-depleted $CD4^+$ responder T cells were isolated from PBMCs from uninfected RM ($n$ = 9) or SM ($n$ = 9) and cocultured with a fixed number of allogeneic irradiated stimulators in the absence or presence of the indicated ratios of autologous Tregs. The *allo*-proliferative response was determined 5 days later by measuring $^3$[H]thymidine uptake; shown for each species are data representative of at least three independent assays. (B) In vitro proliferation of undepleted and CD25-depleted PBMC fractions from $SIV^-$ and $SIV^+$ SM ($n$ = 10) and $SIV^-$ and $SIV^+$ RM ($n$ = 10) was determined by MLR assay. Responders (undepleted or CD25-depleted PBMC fractions) were incubated with irradiated stimulators in a 96-well plate for 5 days at 37°C and 5% $CO_2$. Sixteen hours prior to harvest, plates were pulsed with 1 μCi/well $^3$[H]thymidine. Thymidine uptake was determined, and the precursor frequency was calculated. Data shown are means ± SD, representative of at least three independent assays.

were cocultured with a decreasing number of responder cells (PBMCs with or without Tregs) from uninfected ($n$ = 10) and SIV-infected ($n$ = 10) SM or RM with high VL. The minimum frequency of cells capable of *allo*-MLR response (precursor frequency) was determined. As illustrated by the representative data in Fig. 6B, CD25-depleted cell fractions from both uninfected and SIV-infected SM exhibited similar increases in MLR response, indicated by the ~60% decrease in precursor frequency (note that a decrease in the precursor value denotes an increased number of responding cells). A smaller decrease in precursor frequency (~25%) was noted for uninfected RM. However, no significant change was observed in PBMCs from SIV-infected RM. Collectively, these data therefore suggest that SM have increased functional Treg activity (compared to that for RM), which is maintained following SIV infection; however, not only do RM have a lower Treg functional activity but this functional activity is diminished during chronic infection.

The demonstration of Treg function in these assays prompted us to investigate the role of Tregs in the SIV-specific immune response in SM and RM. The in vitro $CD4^+$ T-cell response to SIV Env and Gag peptide pools was thus determined. PBMC samples from nine uninfected and 12 SIV-infected SM and RM were depleted of Tregs, and by use of immunofluorescent cell count the immune responses to eight pools of SIV Env peptides or eight pools of SIV Gag peptides were determined by measuring the frequencies of IFN-γ-producing $CD4^+$ T cells. Representative data from one animal from each of these two species are shown in Fig. 7. As expected, while $CD4^+$ T cells from both species exhibited a minimal response to the Ova peptide (negative control), concanavalin A and tetanus toxoid induced an increased IFN-γ response, which was markedly increased by the depletion of Tregs. The $CD4^+$ T cells from the SIV-negative RM and SM, also as expected, failed to show any IFN-γ response when tested against a panel of SIV env and gag peptide pools. Of importance was the finding that select pools of SIV env and gag peptides induced IFN-γ production in PBMCs from the SIV-infected RM (Fig. 7, top) and the frequency of responding cells increased significantly (≥2-fold) in the CD25-depleted fractions (Fig. 7, top). In contrast, not only did the $CD4^+$ T cells from the SIV-infected SM fail to respond, removal of the $CD4^+$ $CD25^+$ T cells from an aliquot of the same PBMCs prior to the assay consistently failed to show any detectable increase in the responses (Fig. 7, bottom). Similar results were obtained for the $CD8^+$ T-cell response (data not shown). Thus, the presence of Tregs in PBMCs from RM and SM clearly regulates the magnitude of antigen-specific responses. However, while Tregs from SIV-infected RM dampened the virus-specific T-cell response to select SIV peptides in vitro, the removal of Tregs did not lead to any detectable SIV-specific cellular responses in SIV-infected SM, making it difficult to

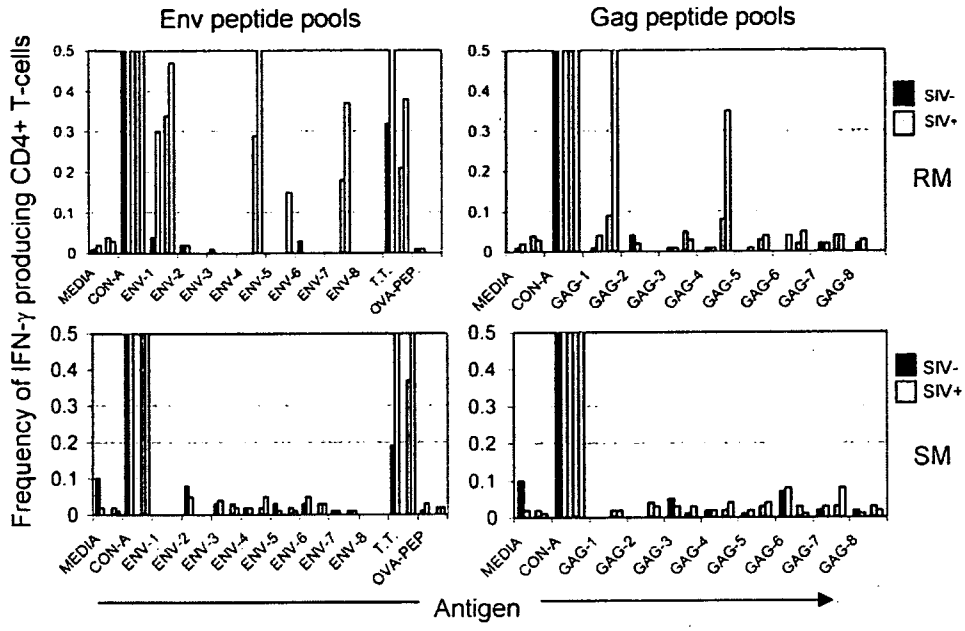


FIG. 7. Effect of Treg depletion on the SIV Env or Gag peptide-specific $CD4^+$ T-cell response in PBMCs from $SIV^-$ or $SIV^+$ RM and SM. Shown are unfractionated PBMCs from $SIV^-$ and $SIV^+$ animals (black and gray bars, respectively) that are paired with their corresponding $CD4^+CD5^+$ T-cell-depleted fraction (white bars). Cells were cultured in the presence of concanavalin A (CON-A) (polyclonal positive control), Ova (OVA-PEP) (negative control), tetanus toxoid (T.T.) (antigen-specific positive control), and eight Env or Gag peptide pools in the presence of brefeldin A. Cells were surface stained for CD4 and then fixed/permeabilized and stained to detect IFN-γ. The frequency of IFN-γ-producing $CD4^+$ T cells was determined by flow cytometry. Shown are data representative of 12 animals of each species. Similar data were obtained for $CD8^+$ T-cell responses (data not shown).

comment on the role of this cell lineage in the virus-specific immune response in the SM species, at least with the pools of peptides that were utilized in this assay.

## DISCUSSION

Support for a role of Tregs in HIV disease progression has kindled interest in defining whether such a role is also present in the SIV-infected nonhuman primate models of AIDS. The rationale here is that a more definitive assignment of a role for this cell lineage in lentiviral infection can be made only by using in vivo manipulative studies of this cell lineage, which is not deemed practical with HIV-infected humans. This determined the purpose of the studies reported herein. Studies with HIV-infected humans thus far have shown that a relative increase in the frequency of Tregs appears to correlate with lower plasma VL and slower disease progression (1, 11, 22, 30). The hypothesis was that Tregs function to regulate the generation of activated $CD4^+$ T cells, which indirectly leads to lower target cells in which the virus could infect and replicate (15, 16, 46), contributing to lower VL and slower disease progression. The main objective of the present study was to identify reagents that would identify Tregs in nonhuman primates, to characterize and compare the levels and functions of Tregs in uninfected and SIV-infected RM and SM, and to determine if observed differences related to the polarized immune responses over the course of infection in these two species. While it is well recognized that immune control is exerted by a number of Treg subsets (natural versus adaptive), such as Tr1, Th3, Th17, and even $CD8^+$ Tregs, the focus of the studies reported herein was the natural $CD4^+$ $CD25^+$ $FoxP3^+$ Tregs that generally develop in the thymus during the early stages of fetal and neonatal T-cell development. It is important to note that the peripheral expansion of $FoxP3^+$-adaptive Tregs has also been suggested previously (7, 8, 19, 36). The characterization of Tregs described here is therefore likely to represent both natural and adaptive subsets of Tregs.

The examination of the kinetics of Tregs during the acute-infection period in RM and SM revealed that divergent Treg responses are exhibited early on by these two species, which may be a critical factor influencing disease outcome. A decrease in the ABS of Tregs occurred during the acute phase in SIV-infected RM, but a larger decline in memory CD4 T cells within the first 3 weeks resulted in a larger Treg:CD4 ratio. A similar trend occurred at 9 weeks p.i., presumably due to the depletion and/or redistribution of memory CD4 T cells. This overall premature Treg induction in SIV-infected RM, which is in agreement with results from a recent study (13), may result in the downregulation of effector T-cell responses at a time when immune control and viral clearance are most important. It may also contribute to an early exhaustion of the generative potential and/or function of Tregs that would be crucial for the prevention or regulation of chronic immune hyperactivation that ultimately results from the persistent viral infection. There was no change in the level of Tregs in SIV-infected SM during the acute phase, and the absence of an early Treg response is in contrast to the rapid immunosuppressive response exhibited by African green monkeys, another natural host of SIV that does not develop AIDS. However, the interpretation of data

from this study is an issue at present since the study was based on characterizing Tregs using the expression of FoxP3 at the message but not the protein level (23). The Treg induction in African green monkeys occurred even earlier than in RM, and it was suggested that this immediate response, although too early to prevent viral replication, may be adequate to prevent chronic immune activation in later stages of infection. In SIV-infected SM, the lack of an early pronounced Treg response may conserve immunological resources necessary for an effective sustained Treg-mediated regulation over the course of infection. It may also be possible that an early Treg induction did occur during the first week of infection prior to our analysis at the 7-day time point.

The analysis of Tregs in animals from the longitudinal study revealed a progressive decline in this cell subset in SIV-infected RM with high plasma VL, but no such decrease occurred in SIV-infected SM. These results were consistent with data from the cross-sectional study, and the decline in Tregs was even more dramatic in the late chronic stage of infection, with the frequency and ABS of Tregs as low as 1.40% ± 1.15% and 2.0% ± 1.4%, respectively. This was also supported by the marked decreases seen in the peripheral and gut-associated lymph node tissues (Fig. 2C). This decline is not unexpected given that the majority of Tregs possess a memory phenotype and a high proportion of this subset expresses CCR5 (L. Picker, unpublished data), the coreceptor used by the virus for cell entry. Thus, the depletion of Tregs over the course of infection is a reflection of the decline in the overall memory CD4 T-cell population, as described before (11, 17, 22). The decline in Tregs could also be attributed to a decrease in CD28 expression following SIV infection (data not shown) since CD28-mediated costimulatory signals have been implicated in the thymic development and peripheral homeostasis of Tregs (44). In contrast to the observed decline in peripheral Tregs in SIV-infected RM, the ABS of Tregs in chronically SIV-infected SM was generally unaltered. It would therefore appear that the chronic immune hyperactivation characteristic of SIV-infected RM might be partly due to the loss of Tregs. In support of this hypothesis, a higher number of Tregs was associated with a lower level of immune activation in chronically SIV-infected RM (Fig. 5). In addition to the observed relationship between Tregs and immune activation, an inverse correlation between Tregs and plasma VL was noted to occur during the chronic state of infection. SIV-infected RM with high VL were found to exhibit higher levels of immune activation and lower numbers of Tregs. This elevated state of activation would provide additional target cells that would further sustain a high VL. Although the observed correlation suggests that high levels of immune activation and VL are a consequence of a decline in Tregs, the data also support the notion that the decrease in Tregs is a consequence of the overall decline in the general CD4 T-cell population due to viral pathogenesis. Indeed, the ability of SIV-infected SM and RM VL controllers to retain Tregs was reflected by the maintenance in total CD4 T cells, and a correlation between the level of Tregs and total CD4 T cells was noted (not shown), in agreement with a recent study involving SM (42). Thus, Tregs may contribute to CD4 T-cell preservation due to its inhibitory effect on immune activation. Conversely, the decline in Tregs in RM VL noncontrollers as a result of viral pathogenesis may be a factor contributing to high levels of immune activation, perpetuating the cycle of viral replication, cell activation, and cell death. Although the data presented herein suggest a positive role for Tregs in SIV infection and/or disease progression, a potential detrimental effect of Tregs via an influence on crucial antiviral immune responses cannot be ruled out. The key to the successful control of viral replication and/or disease progression may perhaps be related to the infection stage at which Tregs exert their regulatory effect, and of course the contribution of other Treg subsets cannot be overlooked.

The decline in the number of Tregs in SIV-infected RM that is suggested by our data does not rule out the effect of SIV-mediated alteration or disruption of Treg function. To address this issue, we first compared the suppressive activities of Tregs isolated from uninfected and SIV-infected SM and RM. In vitro MLR assays suggest that Tregs from uninfected SM generally exhibit a greater degree of suppression than those from RM, and while this potency was maintained in SIV-infected SM, there appeared to be a loss in Treg-mediated suppression in SIV-infected RM. However, the modest enhancement in the response of CD25-depleted cell fractions from SIV-infected RM to select SIV peptide pools suggests that while this cell subset is still functional it most likely plays a limited regulatory role in SIV pathogenesis. Our results therefore suggest that it may be the decline in the number of Tregs and not their loss in function that contributes to the excessive SIV-specific immune response in SIV-infected RM. Since no distinct in vitro response to SIV peptides was observed for PBMCs from SIV-infected SM, which is in agreement with results from a previous study (10), it is difficult to comment on the role of Tregs in the SIV-specific immune response in this species. However, responses to tetanus toxoid were clearly enhanced in the CD25-depleted PBMC fraction, providing support to the notion that the failure was not secondary to a technical issue. In addition, it is important to keep in mind that the SIV peptides being utilized to study the SIV-specific immune response in the SM are based on the SIVmac239 sequence, which may be represented poorly in SM. A more intense study of the effect of SIV infection on Treg function in these animal models, using in vivo depletion of this subset, is under way in our laboratory.

In summary, the present study involved the phenotypic and functional characterization of Tregs from SM and RM and the impact of SIV infection on these parameters. Results show a decline in peripheral Tregs in SIV-infected RM, and the extent of this depletion was found to inversely correlate with both plasma VL and immune activation. In addition to affecting the level of Tregs, SIV infection in RM appears to have a negative impact on Treg function. Thus, while Tregs may contribute to the control of immune activation and VL in RM, the observed trends may simply be attributed to viral pathogenesis. Therefore, the exact nature of this relationship remains to be elucidated. In contrast, both the frequency and the function of Tregs are maintained in SIV-infected SM, leaving their role in disease resistance currently unresolved. Since the regulatory impact of Tregs ultimately depends on their stoichiometry to $CD4^+$ and perhaps total $CD3^+$ effector T cells, a closer examination of the ratio of Tregs to these T-cell populations in both the periphery and the major sites of infection would provide additional insight into the role of Tregs in SIV pathogenesis. The positive effect of ART on Tregs in SIV-infected RM that

is suggested by our data is promising and encourages the design of therapeutic strategies to aid Treg development and/or survival that would limit the immune system damage characteristic of SIV/HIV infection. A recent study suggests that cytotoxic-T-lymphocyte-associated antigen 4 blockade on Tregs in conjunction with ART further reduces vRNA expression in tissues and that this was associated with an increase in virus-specific effector immune responses (but not cell activation, which would favor viral replication) (18). Thus, in addition to increasing Treg levels by using ART, other immune strategies can be employed. It is unclear if the increase in peripheral Tregs observed during ART is a true expansion, a result of T-cell redistribution, or both. The potent immunosuppressive cytokine TGF-β has previously been reported to induce the expression of FoxP3 in $CD4^+$ $CD25^-$ T cells, conferring suppressive activity (8, 14) and possibly thus contributing to Treg development and/or survival. Although previous studies have reported TGF-β induction during the acute phase of SIV infection (13, 23), it would be of interest to assess how TGF-β profiles compare to Treg dynamics over the entire course of infection, particularly in hosts that control VL and do not progress to disease. Analysis of homing markers, such as CCR7 and $\alpha_4\beta_1/\beta_7$ integrins, may address the alternative issue of Treg redistribution.

## ACKNOWLEDGMENTS

This work was supported by NIH RO1 27057 and by AIDS research grants from the Health Sciences Research Grants from the Ministry of Health, Labor and Welfare in Japan.

We are indebted to M. Miller and Gilead Sciences (Foster City, CA) for their generous gift of PMPA for use in these studies.

## REFERENCES

1. **Aandahl, E. M., J. Michaelsson, W. J. Moretto, F. M. Hecht, and D. F. Nixon.** 2004. Human $CD4^+$ $CD25^+$ regulatory T cells control T-cell responses to human immunodeficiency virus and cytomegalovirus antigens. J. Virol. 78:2454–2459.
2. **Annacker, O., R. Pimenta-Araujo, O. Burlen-Defranoux, T. C. Barbosa, A. Cumano, and A. Bandeira.** 2001. CD25+ CD4+ T cells regulate the expansion of peripheral CD4 T cells through the production of IL-10. J. Immunol. 166:3008–3018.
3. **Apoil, P. A., B. Puissant, F. Roubinet, M. Abbal, P. Massip, and A. Blancher.** 2005. FoxP3 mRNA levels are decreased in peripheral blood CD4+ lymphocytes from HIV-positive patients. J. Acquir. Immune Defic. Syndr. 39: 381–385.
4. **Baecher-Allan, C., J. A. Brown, G. J. Freeman, and D. A. Hafler.** 2001. CD4+CD25high regulatory cells in human peripheral blood. J. Immunol. 167:1245–1253.
5. **Baecher-Allan, C., E. Wolf, and D. A. Hafler.** 2005. Functional analysis of highly defined, FACS-isolated populations of human regulatory CD4+CD25+ T cells. Clin. Immunol. 115:10–18.
6. **Bostik, P., E. S. Noble, A. E. Mayne, L. Gargano, F. Villinger, and A. A. Ansari.** 2006. Central memory CD4 T cells are the predominant cell subset resistant to anergy in SIV disease resistant sooty mangabeys. AIDS 20:181–188.
7. **Chatenoud, L., and J. F. Bach.** 2006. Adaptive human regulatory T cells: myth or reality? J. Clin. Investig. 116:2325–2327.
8. **Chen, W., W. Jin, N. Hardegen, K. J. Lei, L. Li, N. Marinos, G. McGrady, and S. M. Wahl.** 2003. Conversion of peripheral CD4+CD25− naive T cells to CD4+CD25+ regulatory T cells by TGF-beta induction of transcription factor Foxp3. J. Exp. Med. 198:1875–1886.
9. **Cobb, B. S., A. Hertweck, J. Smith, E. O'Connor, D. Graf, T. Cook, S. T. Smale, S. Sakaguchi, F. J. Livesey, A. G. Fisher, and M. Merkenschlager.** 2006. A role for Dicer in immune regulation. J. Exp. Med. 203:2519–2527.
10. **Dunham, R., P. Pagliardini, S. Gordon, B. Sumpter, J. Engram, A. Moanna, M. Paiardini, J. N. Mandl, B. Lawson, S. Garg, H. M. McClure, Y. X. Xu, C. Ibegbu, K. Easley, N. Katz, I. Pandrea, C. Apetrei, D. L. Sodora, S. I. Staprans, M. B. Feinberg, and G. Silvestri.** 2006. The AIDS resistance of naturally SIV-infected sooty mangabeys is independent of cellular immunity to the virus. Blood 108:209–217.
11. **Eggena, M. P., B. Barugahare, N. Jones, M. Okello, S. Mutalya, C. Kityo, P. Mugyenyi, and H. Cao.** 2005. Depletion of regulatory T cells in HIV infection is associated with immune activation. J. Immunol. 174:4407–4414.
12. **Epple, H. J., C. Loddenkemper, D. Kunkel, H. Troger, J. Maul, V. Moos, E. Berg, R. Ullrich, J. D. Schulzke, H. Stein, R. Duchmann, M. Zeitz, and T. Schneider.** 2006. Mucosal but not peripheral FoxP3+ regulatory T cells are highly increased in untreated HIV infection and normalize after suppressive HAART. Blood 108:3072–3078.
13. **Estes, J. D., Q. Li, M. R. Reynolds, S. Wietgrefe, L. Duan, T. Schacker, L. J. Picker, D. I. Watkins, J. D. Lifson, C. Reilly, J. Carlis, and A. T. Haase.** 2006. Premature induction of an immunosuppressive regulatory T cell response during acute simian immunodeficiency virus infection. J. Infect. Dis. 193: 703–712.
14. **Fantini, M. C., C. Becker, G. Monteleone, F. Pallone, P. R. Galle, and M. F. Neurath.** 2004. Cutting edge: TGF-beta induces a regulatory phenotype in CD4+CD25− T cells through Foxp3 induction and down-regulation of Smad7. J. Immunol. 172:5149–5153.
15. **Finzi, D., M. Hermankova, T. Pierson, L. M. Carruth, C. Buck, R. E. Chaisson, T. C. Quinn, K. Chadwick, J. Margolick, R. Brookmeyer, J. Gallant, M. Markowitz, D. D. Ho, D. D. Richman, and R. F. Siliciano.** 1997. Identification of a reservoir for HIV-1 in patients on highly active antiretroviral therapy. Science 278:1295–1300.
16. **Finzi, D., and R. F. Siliciano.** 1998. Viral dynamics in HIV-1 infection. Cell 93:6314–6319.
17. **Grossman, Z., M. Meier-Schellersheim, W. E. Paul, and L. J. Picker.** 2006. Pathogenesis of HIV infection: what the virus spares is as important as what it destroys. Nat. Med. 12:289–295.
18. **Hryniewicz, A., A. Boasso, Y. Edghill-Smith, M. Vaccari, D. Fuchs, D. Venzon, J. Nacsa, M. R. Betts, W. P. Tsai, J. M. Heraud, B. Beer, D. Blanset, C. Chougnet, I. Lowy, G. M. Shearer, and G. Franchini.** 2006. CTLA-4 blockade decreases TGF-β, IDO and viral RNA expression in tissues of SIVmac251-infected macaques. Blood 108:3834–3842.
19. **Itoh, M., T. Takahashi, N. Sakaguchi, Y. Kuniyasu, J. Shimizu, F. Otsuka, and S. Sakaguchi.** 1999. Thymus and autoimmunity: production of CD25+CD4+ naturally anergic and suppressive T cells as a key function of the thymus in maintaining immunologic self-tolerance. J. Immunol. 162: 5317–5326.
20. **Jonuleit, H., E. Schmitt, M. Stassen, A. Tuettenberg, J. Knop, and A. H. Enk.** 2001. Identification and functional characterization of human CD4(+)CD25(+) T cells with regulatory properties isolated from peripheral blood. J. Exp. Med. 193:1285–1294.
21. **Kaur, A., R. M. Grant, R. E. Means, H. McClure, M. Feinberg, and R. P. Johnson.** 1998. Diverse host responses and outcomes following simian immunodeficiency virus SIVmac239 infection in sooty mangabeys and rhesus macaques. J. Virol. 72:9597–9611.
22. **Kinter, A. L., M. Hennessey, A. Bell, S. Kern, Y. Lin, M. Daucher, M. Planta, M. McGlaughlin, R. Jackson, S. F. Ziegler, and A. S. Fauci.** 2004. CD25(+)CD4(+) regulatory T cells from the peripheral blood of asymptomatic HIV-infected individuals regulate CD4(+) and CD8(+) HIV-specific T cell immune responses in vitro and are associated with favorable clinical markers of disease status. J. Exp. Med. 200:331–343.
23. **Kornfield, C., M. J. Y. Ploquin, I. Pandrea, A. Faye, R. Onanga, C. Apetrei, V. Poaty-Mavoungou, P. Rouquet, J. Estaquier, L. Mortara, J. F. Desoutter, C. Butor, R. L. Grand, P. Roques, F. Simon, F. Barre-Sinoussi, O. M. Diop, and M. C. Muller-Trutwin.** 2005. Antiinflammatory profiles during primary SIV infection in African green monkeys are associated with protection against AIDS. J. Clin. Investig. 115:1082–1091.
24. **Kuroda, M. J., J. E. Schmitz, W. A. Charini, C. E. Nickerson, M. A. Lifton, C. I. Lord, M. A. Forman, and N. L. Letvin.** 1999. Emergence of CTL coincides with clearance of virus during primary simian immunodeficiency virus infection in rhesus monkeys. J. Immunol. 162:5127–5133.
25. **Levings, M. K., R. Sangregorio, and M. G. Roncarolo.** 2001. Human CD25+CD4+ T regulatory cells suppress naive and memory T-cell proliferation and can be expanded *in vitro* without loss of function. J. Exp. Med. 193:1295–1302.
26. **Liu, W., A. L. Putnam, Z. Xu-Yu, G. L. Szot, M. R. Lee, S. Zhu, P. A. Gottlieb, P. Kapranov, T. R. Gingeras, B. F. D. St. Groth, C. Clayberger, D. M. Soper, S. F. Ziegler, and J. A. Bluestone.** 2006. CD127 expression inversely correlates with FoxP3 and suppressive function of human CD4+ T reg cells. J. Exp. Med. 203:1701–1711.
27. **McHugh, R. S., M. J. Whitters, C. A. Piccirillo, D. A. Young, E. M. Shevach, M. Collins, and M. C. Byrne.** 2002. CD4(+)CD25(+) immunoregulatory T cells: gene expression analysis reveals a functional role for the glucocorticoid-induced TNF receptor. Immunity 16:311–323.
28. **Nakamura, K., A. Kitani, and W. Strober.** 2001. Cell contact-dependent immunosuppression by CD4(+)CD25(+) regulatory T cells is mediated by cell surface-bound transforming growth factor beta. J. Exp. Med. 194:629–644.

28a. **National Research Council.** 1996. Guide for the care and use of laboratory animals. National Academy Press, Washington, DC.

29. **Nilsson, J., A. Boasso, P. A. Velilla, R. Zhang, M. Vaccari, G. Franchini, G. M. Shearer, J. Andersson, and C. Chougnet.** 2006. HIV-1 driven regula-